

RESEARCH

Open Access



Ductility Design of Reinforced Very-High Strength Concrete Columns (100–150 MPa) Using Curvature and Energy-Based Ductility Indices

Shanaka Kristombu Baduge* , Priyan Mendis, Tuan Duc Ngo* and Massoud Sofi

Abstract

The paper aims to develop theoretical expressions for the ductility design of very-high strength concrete (VHSC) (> 100 MPa) columns using curvature and a new flexural energy-based ductility approach. Eventually, the study aims to evaluate the feasibility of VHSC columns for different ductility classes, considering the limitation of providing a higher volume of transverse reinforcement due to possible steel congestion in the construction phase. An analytical program based on the experimental stress–strain relationship of confined VHSC, which is validated using experimental programs on VHSC columns, is used to evaluate the ductility of VHSC columns for different parameters such as axial load ratio, confinement pressure, longitudinal steel ratio, yield strength of transverse steel, cover area and compressive strength of concrete. The theoretical curvature ductility and flexural rotation-based energy ductility of 3200 rectangular columns were evaluated using the analytical program. Using curvature ductility and the new flexural rotation-based energy ductility for different parameters, a regression analysis is carried out to develop expressions for the ductility design of VHSC columns up to 150 MPa. Using the new definition of energy-based ductility, a new expression is developed for limited ductility design of VHSC; and it is concluded that the new approach reduces the required amount of steel confinement due to an increase in the energy ductility of VHSC at higher axial load ratios and higher strengths. The studies show that reinforced VHSC can be used for structures with nominal ductility demands.

Keywords: very-high strength concrete, ductility design, transverse reinforcement, curvature ductility, energy ductility, moment–curvature analysis, tall building

1 Introduction

Instead of designing structures elastically to withstand lateral forces from severe and infrequent earthquakes, designing structures for lower force levels and higher ductility is a widely accepted practice in performance-based design. Ductility enables the structure to undergo large cyclic deformation whilst sustaining the load carrying capacity and dissipating energy in hysteresis cycles. However, the formation of hinges in columns is

undesirable in structural engineering as it can cause a weak storey mechanism, as well as instability in gravity retaining structures. In performance-based design, hinges are desirable in beams, resulting in a beam-sway mechanism. Mixed-sway mechanisms, where hinges form in columns and beams, are allowed when structures are prone to low-seismic conditions. Interestingly, some earthquakes (e.g. Kobe, Japan in 1995; and Northridge, USA in 1994) and analysis by researchers (Bayrak 1995; Mitchell and Paultre 1994) showed that the formation of plastic hinges in columns is possible at locations other than the first storey due to higher mode effects. Thus, columns should be detailed to ensure plastic hinges have at least the minimum of anticipated ductility during ground motion.

*Correspondence: kasun.kristombu@unimelb.edu.au;
dtngo@unimelb.edu.au
Department of Infrastructure Engineering, The University of Melbourne,
VIC 3052, Australia
Journal information: ISSN 1976-0485 / eISSN 2234-1315

Lateral reinforcement being used to for shear resistance, confinement and prevent buckling of longitudinal reinforcement. In general, adequate ductility of concrete structures can be achieved by confining the concrete core using lateral reinforcement. Therefore, in ductility design of concrete members, lateral steel is designed to provide adequate ductility while considering the parameters such as axial-load ratio, longitudinal steel ratio, yield strength of transverse steel, cover area and compressive strength of concrete. Thus, knowing the amount of ductility for the given confinement level, or conversely, the required confinement level (i.e. the required transverse reinforcement) for the anticipated ductility level is essential in structural engineering.

The ductility of concrete columns is quantified using the deformation at the yield moment and the ultimate deformation, which is commonly defined as the deformation at 80% of the maximum peak moment. The yield moment is defined as the moment at yielding of concrete or steel. The type of deformation can be displacement, curvature or rotation. Generally, the ductility of structural members is measured using the curvature ductility (μ_ϕ) and the displacement ductility (μ_d) (Mendis and Kovacic 1999; Park and Paulay 1975; Paultre and Légeron 2008; Watson et al. 1994), and these definitions are used to develop the guidelines for ductility design. Foster (1999) proposed an energy-based ductility index (I_{10}) to capture the plastic energy of columns subjected to axial and flexural deformation. These available energy-based ductility definitions have been used in codes of practice to develop guidelines for ductility design (AS 3600 2009; Foster and Attard 1997; Kristombu Baduge 2016). Kristombu Baduge (2016) proposed a flexural rotation-based energy ductility index (E_θ) that can represent the flexural energy of structural members because the existing indices cannot capture the higher flexural rotation energy of VHSC members.

The ductility of concrete members can be evaluated using analytical nonlinear full-range moment–curvature analysis. However, such rigorous analysis cannot be effectively used in structural design practice due to its complexity and computational time. Therefore, it is necessary to develop simple design equations to determine the required amount of transverse steel for the anticipated ductility level whilst considering associated parameters such as strength, axial load level, cover and longitudinal steel ratio. Codes of practice (AS 3600 2009; CSA 23.3 2004; EC 8 2004b; NZS 3101.1 2006) and research (Bai and Au 2013; Kwan and Ho 2010; Mendis 2001a, b; Paultre and Légeron 2008; Saatcioglu and Razvi 2002; Sheikh and Houry 1997; Watson et al. 1994) have been developed to calculate the amount of transverse reinforcement needed to gain the required ductility level (displacement

or curvature). The guidelines from the codes of practice and the researchers are based on the analytical non-linear moment–curvature behaviour of reinforced concrete members.

A comprehensive literature review on the ductile design of high-strength concrete (HSC) concluded that neither existing codes of practice nor research methods do not provide any ductile design guidelines for compressive strengths greater than 100 MPa and 120 MPa, respectively; even though economically and technically feasible VHSC with compressive strengths of up to 150 MPa can be produced and effectively used in many structures such as long-span bridges and columns of tall buildings which needs higher compressive strengths (Kristombu Baduge et al. 2013, 2015). Therefore, developing theoretical guidelines for economical ductility design of VHSC with compressive strengths up to 150 MPa is vital to enable using of VHSC columns.

2 Summary of Ductility Design of Reinforced Concrete Columns

Paultre and Légeron (2008) developed mathematical expressions for the ductility design of medium and high-ductile structures using nonlinear moment–curvature analysis and experimental results. The design guidelines were developed for columns with compressive strengths of up to 130 MPa and transverse steel yield strengths of up to 1400 MPa. The method proposed by Paultre and Légeron (2008) is used in CSA (2004). Kwan and Ho (2010) carried out a parametric study on the ductility of beams and columns by numerically analysing nonlinear moment–curvature curves. The limited ductility level is defined as $\mu_\phi = 3.32$, which is equal to or similar to a 30 MPa Normal Strength Concrete (NSC) beam detailed according to the minimum requirements of codes. The effects of varying several parameters are studied: concrete strength from 40 to 100 MPa; axial load level from 0.1 to 0.6; steel yield strength from 250 to 600 MPa; confinement pressure from 0 to 4 MPa; and compression and tension steel ratios from 0 to 2% and 0.4 to 6% of the balanced steel ratio, respectively. Watson et al. (1994) developed design equations for ductile and medium ductile structures, assuming that a curvature ductility of 10 and 20 is adequate for medium-ductile and ductile structures, respectively. The equations are based on analytical full-range moment–curvature analysis, which considers the cyclic effects of steel and concrete. However, the analytical method is based on the stress–strain behaviour proposed by Mander et al. (1988), which is only valid for NSC. Therefore, the validity of equations by Watson et al. (1994) for strengths greater than 50 MPa is uncertain, even though these equations are used by NZS 3101.1 (2006) for strengths of up to 70 MPa. Mendis and Kovacic

(1999) proposed a simple formula for the nominal ductility design of HSC columns using nonlinear moment curvature analysis.

Even though curvature ductility is generally used to develop guidelines for ductility design, Foster (1999) proposed an energy-based ductility index (I_{10}) for ductility design. The index, which captures the plastic energy stored in the structural element, is obtained according to the method proposed by ASTM C 1018 (1992). The study Foster (1999) suggested that curvature ductility levels of an equivalent 50 MPa column detailed according to the minimum requirements of AS (2009) is adequate for nominal ductility design due to the fact that AS (2009) does not specify any additional confinement to achieve adequate ductility for compressive strengths of 50 MPa or less.

Table 1 concludes that researchers have used different definitions for ductility and different quantities for the ductility design of high strength concrete, which are dependent on seismic demands in the region. NZS 3101.1 (2006) considers three ductility classes: nominal ductile structures (NDS), limited ductile structures (LDS) and ductile structures (DS). CSA (2004) gives detailed guidelines for conventional ductile structures (CDS), moderate ductile structures (MDS) and ductile structure (DS). AS (2009) provides guidelines for ordinary moment resisting frames (OMRF), intermediate moment resisting frames (IMRF) and special moment resisting frames (SMRF). For SMRF, AS (2009) refers to NZS 3101.1 (2006) to determine confinement requirements. EC 8 (2004a) defines guidelines for ductility class low (DCL), ductility class medium (DCM) and ductility class high (DCH). The nominal ductility design in AS (2009) is based on the energy approach proposed by Foster (1999) and it suggests an energy ductility level of 5.6, which is similar to the ductility level of a 50 MPa column detailed according to the minimum requirements of AS (2009).

Generally, the ductility of structures or members is classified into three categories by codes of practice as

shown in Table 2: low ductile, medium ductile and ductile structures. Table 2 summarises the required ductility levels specified by major codes of practice around the world. However, the ductility levels specified in the guidelines do not have any consistency and are dependent on the anticipated seismic levels in the region.

3 Theoretical Method to Predicting the Ductility of VHSC Columns

Curvature and energy ductility of columns can be analytically predicted using a full-range moment–curvature relationship and the material constitutive behaviour and incorporating material failure criteria. Researchers (Bai and Au 2013; Kwan and Ho 2010; Mendis et al. 2000; Paultre and Légeron 2008) used analytical programs to develop guidelines for ductility design. In this study, an analytical program, which uses a layered representation of the confined core and unconfined cover with relevant material models, is developed using MATLAB (MATLAB User’s Guide 1998) mathematical software to predict the flexural behaviour of columns. The concrete, longitudinal steel and transverse steel are assigned to suitable material models. The program considers possible spalling of cover concrete, buckling of longitudinal steel and hoop fracture in the incremental analysis. The following sections explain the material constitutive models, failure criteria and the algorithm of the analytical program. Even though the study aims on developing ductility design guidelines for rectangular column sections the methodology can be used for circular columns sections.

3.1 Algorithm for the Numerical Analysis of Nonlinear Moment–Curvature Behaviour

The following basic assumptions are established in the analytical program:

1. The plane section remains plane throughout the loading.

Table 1 Summary of ductile design guidelines for HSC and VHSC.

Researcher	Compressive strength (max), MPa	Ductility class	Material model for concrete	Curvature/energy ductility
Mendis et al. (2000)	100	Nominal ductility	Modified-Scott model (Mendis et al. 2000)	μ_ϕ = ductility of an equivalent 50 MPa column detailed according to minimum requirements of AS 3600
Kwan and Ho (2010)	130	Nominal ductility	Model by Légeron and Paultre (2003)	μ_ϕ = 3.14-similar to curvature ductility of 30 MPa column
Foster (1999)	100	Nominal ductility	–	I_{10} = 5.6, similar to energy ductility of 50 MPa column detailed according to the minimum requirements of AS 3600
Paultre and Légeron (2008)	120	Moderate to high ductility	Model by Légeron and Paultre (2003)	μ_ϕ = 10 and 16, respectively

Table 2 Summary of ductile design guidelines in codes of practice.

Code	Ductility index	Compressive strength limit	Ductility LEVEL			Lateral reinforcement requirement for ductility		
			Category I	Category II	Category III	Category I	Category II	Category III
AS 3600 (2009)	Energy-based ductility	100 MPa	OMRF 2.0	IMRF 3.0	– Refer to NZS 1170.5 (2004)	Yes	Yes	No
CSA (2004)	Curvature and displacement ductility	80/80 ^a MPa	CDS 1.5	MDS 2.5	DS 4.0	No	Yes	Yes
ACI 318 (2011)	Curvature and displacement ductility	No limit ^b	OMRF 1.0	IMRF 1.7	SMRF 2.7	Yes	Yes	Yes
NZS 3101.1 (2006)	Curvature ductility	100/70 ^a MPa	NDS 1.25	LDS 3.0	DS 6.0	Yes	Yes	Yes
EC 8 (2004a) and EC 2 (2004)	Curvature and displacement ductility	100 MPa	DCL 1.5	DCM 3.0	DCH 4.5	No	No	Yes

^a For ductile elements in seismic design.

^b Concrete strength limited in some design equations.

2. There is no bond slip between the rebar and concrete.
3. Tensile forces in the concrete section are negligible.

Figure 1 illustrates a typical section with a breadth of b and width of h , with tensile reinforcement (A_{st}) and compressive reinforcement (A_{sc}) provided at d_2 and d_1 from the top of the section, respectively. Also, d_n is the depth of the neutral axis (NA) for a given curvature (ϕ) at the extreme compression fibre. The sign of d_n considered as positive if d_n is below the extreme compression fibre.

The complete nonlinear moment–curvature behaviour is analysed by imposing an incremental prescribed curvature starting from zero and predicting the moment capacity for the given curvature. For a prescribed curvature, an arbitrary neutral axis depth is assumed. If x is the distance from the top to any arbitrary fibre of the section, the following equation can be used to evaluate the strain at any location using strain compatibility:

$$\epsilon_x = \phi(d_n - x) \tag{1}$$

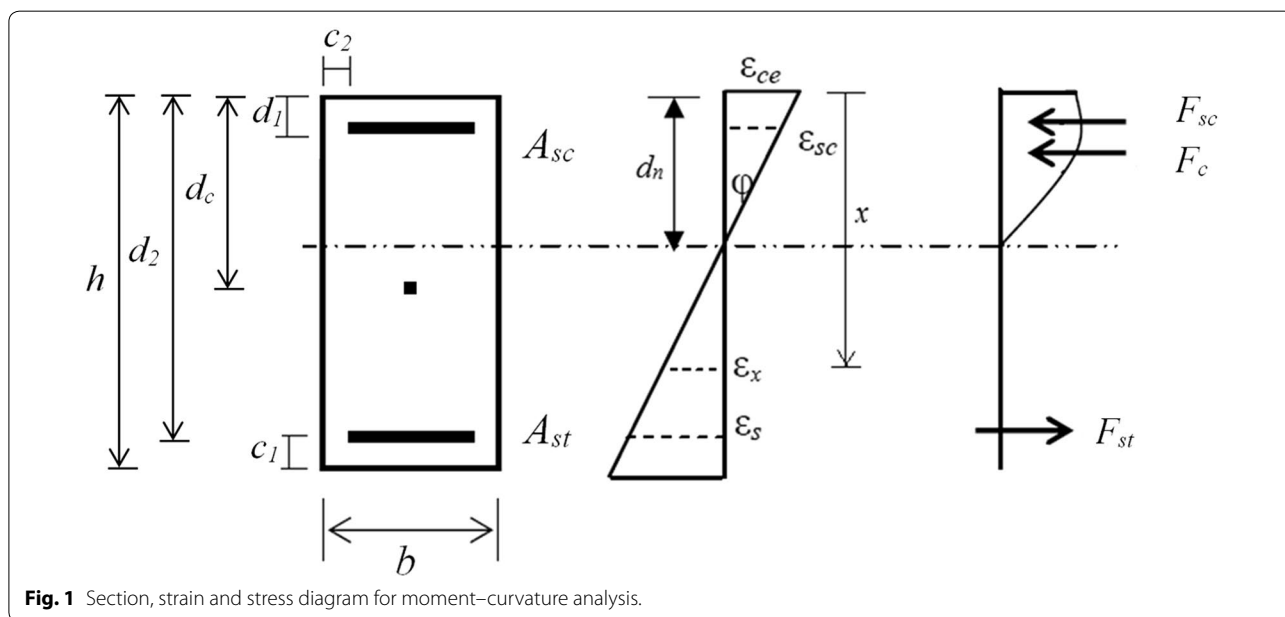


Fig. 1 Section, strain and stress diagram for moment–curvature analysis.

Using Eq. (1), strains developed in the different materials are calculated. Dependent on the location of the NA, the strain can be positive or negative. Consequently, stress and forces will be positive and negative. Even though Fig. 1 shows a typical case where NA is within the section, the equation valid where NA outside the NA. For example, the compressive strain at the extreme compression fibre (ϵ_{ce}), the compressive strain at the top reinforcement (ϵ_{sc}) and the tensile strain at the bottom reinforcement (ϵ_{st}) can be written using the following equations, respectively:

$$\epsilon_{ce} = \phi d_n \tag{2}$$

$$\epsilon_{sc} = \phi(d_n - d_1) \tag{3}$$

$$\epsilon_{st} = \phi(d_n - d_2) \tag{4}$$

Then, the corresponding stress distributions throughout the section for confined concrete, unconfined concrete, tensile steel and compression steel (σ_{cc} , σ_{cu} , σ_{st} and σ_{sc} , respectively) are calculated using the respective material stress–strain behaviours. The total force from confined (concrete core), unconfined concrete (cover concrete) and steel are evaluated by numerical integration as follows:

$$P = \int_0^h \sigma_{cu}(x)b dx + \int_{c_1}^{h-c_1} [\sigma_{cc}(x) - \sigma_{cu}(x)](b - 2c_2)dx + A_{sc}\sigma_{sc} + A_{st}\sigma_{st} \tag{5}$$

where c_1 and c_2 are lengths of cover, as defined in Fig. 1.

Using force equilibrium for the section, the validity of the assumed neutral axis depth is evaluated such that the resultant force (P) is zero. An iterative solver is used to find the accurate neutral axis depth under the condition that force equilibrium is established. Having determined the neutral axis depth, the moment capacity (M) is evaluated using the moment equilibrium of the section about the centroid (d_c) as follows:

$$M = \int_0^h \sigma_{cu}(x)b(d_c - x)dx + \int_{c_1}^{h-c_1} [\sigma_{cc}(x) - \sigma_{cu}(x)](b - 2c_2)(d_c - x)dx + A_{sc}\sigma_{sc}(d_c - d_1) + A_{st}\sigma_{st}(d_c - d_2) \tag{6}$$

The prescribed curvature and the corresponding moment capacity is a point on the full-range moment–curvature curve. This method is repeated with incremental curvature until the following conditions are encountered:

1. The moment is less than 25% of the peak moment capacity, or

2. Load carrying capacity of the longitudinal steel drops by 25% due to buckling of the longitudinal steel, or
3. Fracture of lateral or longitudinal steel.

3.2 Material Constitutive Behaviour

For VHSC, the following models are used in the analytical program.

3.2.1 Unconfined Concrete

Previous studies shows that unconfined VHSC behave different to Normal Strength Concrete (NSC) (Kristombu Baduge et al. 2018; Lee et al. 2018). Even though researchers have proposed various types of stress–strain models for unconfined HSC based on extensive experimental programs, only a few stress–strain models, such as those proposed by (Attard and Setunge 1996; Candappa et al. 1999; Légeron and Paultre 2003; Razvi and Saatcioglu 1999; Samani and Attard 2012) can predict the constitutive behaviour of concrete with strengths greater than 100 MPa. The stress–strain model developed by Légeron and Paultre (2003) is valid up to 130 MPa and Kristombu Baduge (2016) used this model for unconfined VHSC up to 150 MPa with some modifications. Thus, the model proposed by Légeron and Paultre (2003) is selected to model the unconfined behaviour of VHSC with a modified peak strain and modulus of elasticity.

3.2.2 Confined Concrete

The stress–strain models for confined VHSC proposed by researchers such as (Attard and Setunge 1996; Cusson and Paultre 1995; Razvi and Saatcioglu 1999) are valid up to compressive strengths of 125–130 MPa, and are developed assuming that the behaviour is governed by the confining effects from lateral reinforcement only. Previous experimental studies (Kristombu Baduge et al. 2018b, c) showed that the confined behaviour of VHSC is dependent on confinement from the lateral reinforcement, dowelling action of the lateral and longitudinal reinforcement, and the concrete shear force at the failure plane, as shown in Fig. 2. However, existing models are derived considering confinement effects only and the experimental program by Kristombu Baduge (2016) showed that incorporating the doweling action and shear force at the failure plane (Fig. 2) due to cohesion and friction can predict the results more accurately.

The model is developed for compressive strengths in the range of 120–160 MPa and is validated using experimental results (Kristombu Baduge 2016). The stress–strain model proposed by Kristombu Baduge (2016) was used in the analytical program (see Fig. 3b). Further details of the new stress–strain model can be found in elsewhere (Kristombu Baduge et al. 2018a). The

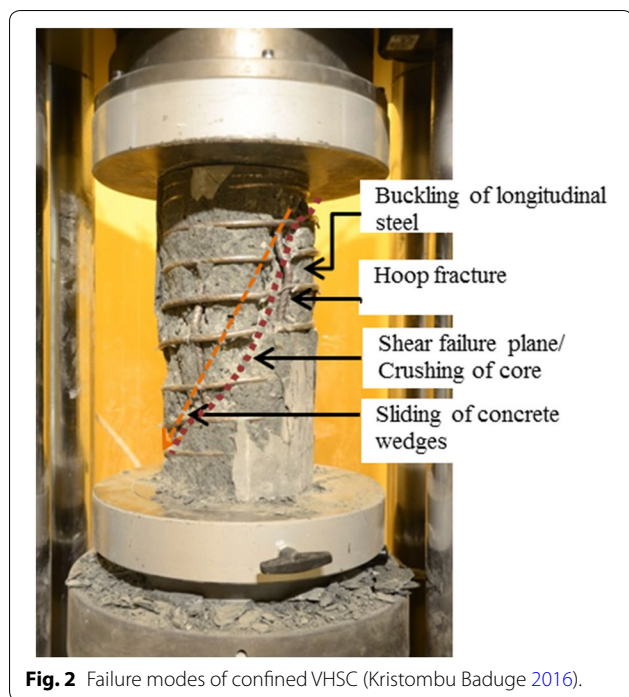


Fig. 2 Failure modes of confined VHSC (Kristombu Baduge 2016).

stress–strain model for confined concrete is valid for circular sections so that the method proposed in the study can be used to predict the moment–curvature relationship of circular columns. The parameters for the material constitute models can be found in Kristombu Baduge et al. (2018).

3.2.3 Steel

The stress–strain model proposed by Samra (1990) is used for the analysis of the steel reinforcement. The experimental program by Kristombu Baduge (2016) on confined VHSC samples showed that the stress–strain behaviour of the confined core is related to the buckling of longitudinal steel and hoop fracture. Similarly, Mendis et al. (2000) showed that it is important to consider hoop fracture and buckling of longitudinal reinforcement in the prediction of accurate moment–curvature behaviour.

First, hoop fracture can be associated with the ultimate strain of confined concrete due to an abrupt reduction in the capacity and subsequent failure of hoops due to sudden load transfer. Equation (7) proposed by Wei and Wu (2014) is used to calculate the ultimate strain.

$$\epsilon_{cu} = \epsilon_{cc} + 900\epsilon_{co}\epsilon_{su} \left(\frac{f_r}{f_{co}} \right) \tag{7}$$

where ϵ_{cc} and ϵ_{co} are the peak strain of confined and unconfined concrete, respectively, f_r is effective confinement pressure, f_{co} is compressive strength of concrete.

Buckling of longitudinal steel bars can occur due to higher axial compression after the spalling of cover concrete (Bae 2006, Chapter 6; Bayrak and Sheikh 2001; Kristombu Baduge 2016; Mander et al. 1984). The tensile and compressive behaviour of a steel bar is different when the steel is subjected to buckling. Therefore, accurate modelling of the buckling and stress–strain behaviour of steel is important to predict the post-peak behaviour of the moment–curvature relationship. Researchers such as (Bae et al. 2005; Bayrak and Sheikh 2001; Bresler and Gilbert 1961; Mau 1990; Mau and El-Mabsout 1989; Papia and Russo 1989; Scribner 1986) developed the stress–strain behaviour of steel under compression and incorporated inelastic buckling. The method proposed by Bae et al. (2005) is used in the analytical program.

Figure 3c presents the nonlinear full-range moment–curvature behaviour predicted with the MATLAB analytical program for a square column under axial load ratios corresponding to 0.1 to 0.5. For this column, the following parameters were used: $\rho_l=0.17$, $f_r=4$ MPa, $f_c=130$ MPa: ρ_l is longitudinal steel ratio, f_r is confinement pressure and f_c is compressive strength of concrete.

3.3 Method to Calculate Ductility of VHSC Columns

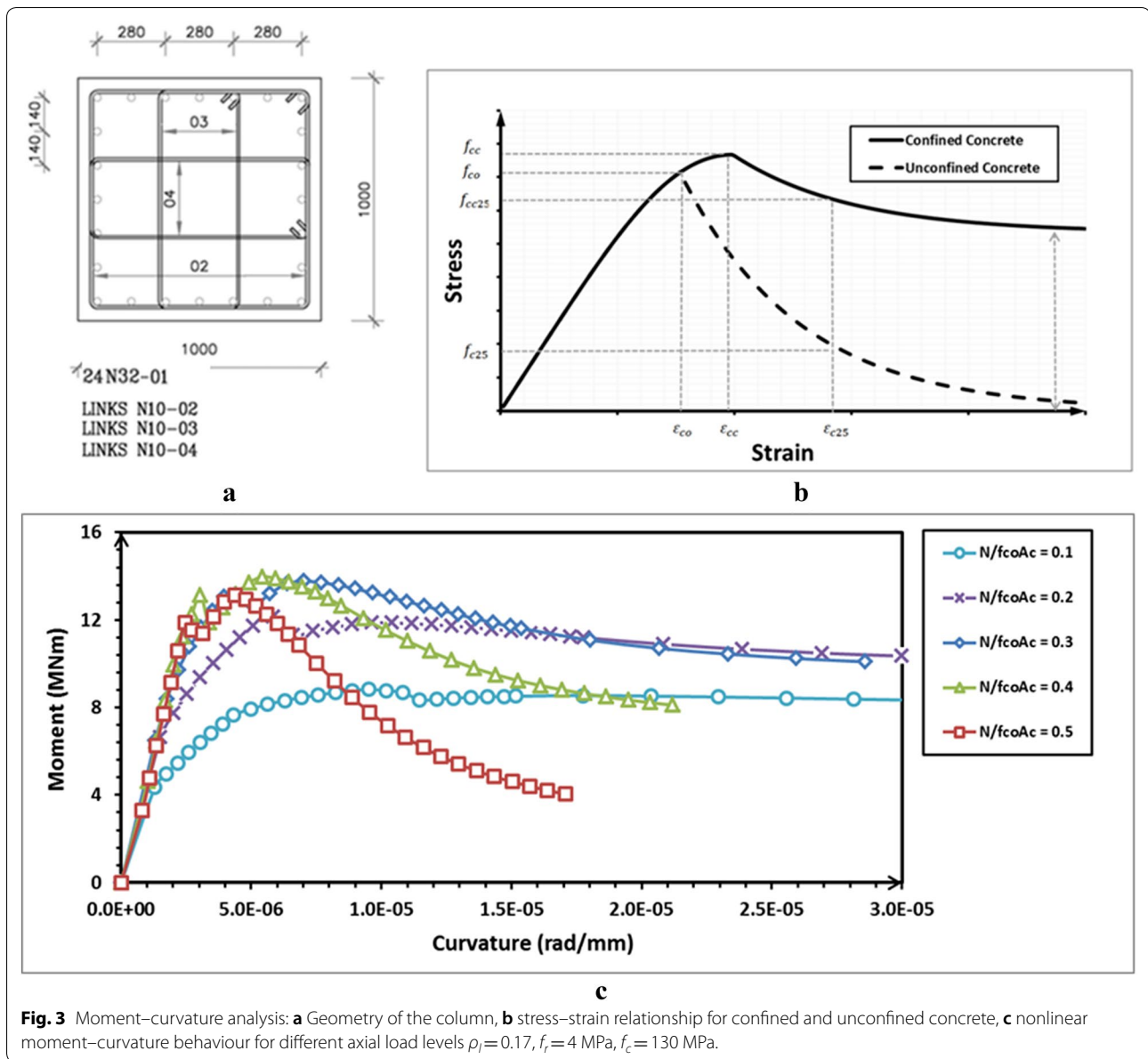
3.3.1 Curvature Ductility of VHSC Columns

Using the full-range moment–curvature diagram, the curvature ductility can be evaluated. Figure 4 illustrates the curvature ductility curve of VHSC columns with a similar geometry to that shown in Fig. 3a. The columns have a compressive strength of 130 MPa, different axial load levels ($P/f_c A_c=0.1, 0.2, 0.3, 0.4$ and 0.5), and different confinement levels ($f_r=1, 2, 3$ and 4 MPa).

3.3.2 Energy-Based Ductility of VHSC Columns

Kristombu Baduge (2016) showed that the curvature ductility cannot represent the increase in the plastic energy of VHSC columns along with an increase in the peak moment (Fig. 5) due to the confinement effect, higher strength and higher axial load levels. Plastic energy is related to the energy dissipation characteristics during cyclic deformation in an earthquake event. Incorporating the plastic strain energy into ductility indices is vital for VHSC members because they dissipate relatively large energy compared to a normal strength concrete member of the same ductility (Elmshawi 2008) as shown in Fig. 5, and can thereby have higher energy dissipation characteristics.

Considering the importance of incorporating plastic energy into the ductility index, the importance of flexural deformation in an earthquake event and the load sustaining capacity of columns, (Kristombu Baduge 2016) proposed the flexural rotation-based energy ductility index (E_θ) to evaluate the ductility of VHSC columns.



The expression given by Eq. (8), based on the rotational energy of flexural deformation, is proposed for the flexural rotation-based energy ductility index, E_θ :

$$E_\theta = \frac{\int_0^{\theta_u} M d\theta}{\int_0^{\theta_y} M d\theta} \tag{8}$$

where M and θ are the moment and rotation of the moment-rotation graph, respectively; θ_y is the yield rotation; and θ_u is the rotation at ϕ_u . The moment-rotation behaviour can be predicted using the moment-curvature relationship once the plastic hinge length and height of the column are known. The moment-rotation graph can

be generated using the moment-curvature graph for a double-curvature column. The total rotation due to flexure deformation can be calculated by adding elastic rotation and plastic rotation as given in Eq. (9) and Eq. (10), respectively which proposed by Elmenhawhi (2008): for $\theta_y \geq \theta$

$$\theta = \phi L/6 \tag{9}$$

where θ is rotation of a prismatic element with double curvature, ϕ is curvature, and L is length of the column.

Assuming the plastic curvature is constant and uniformly distributed over the plastic hinge length, L_p ; for $\theta_y < \theta$

$$\theta = (\phi - \phi_y)L_p \tag{10}$$

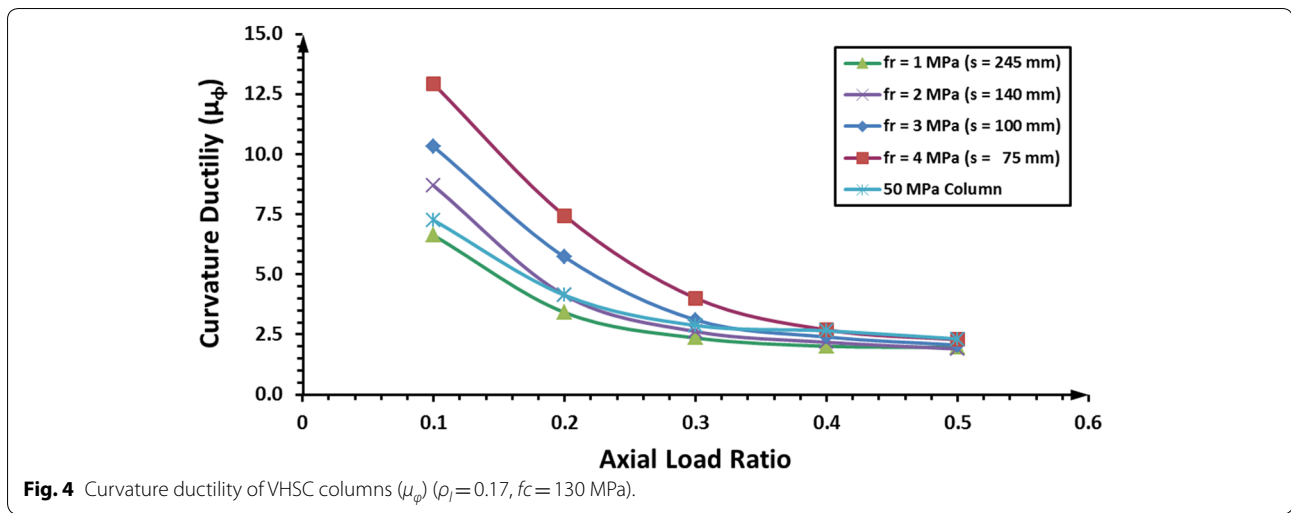


Fig. 4 Curvature ductility of VHSC columns (μ_{ϕ}) ($\rho_l = 0.17$, $f_c = 130$ MPa).

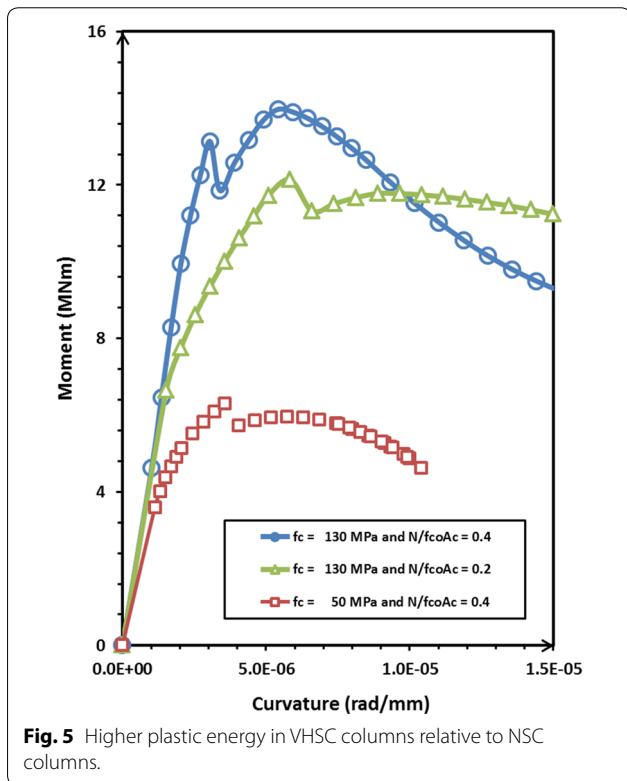


Fig. 5 Higher plastic energy in VHSC columns relative to NSC columns.

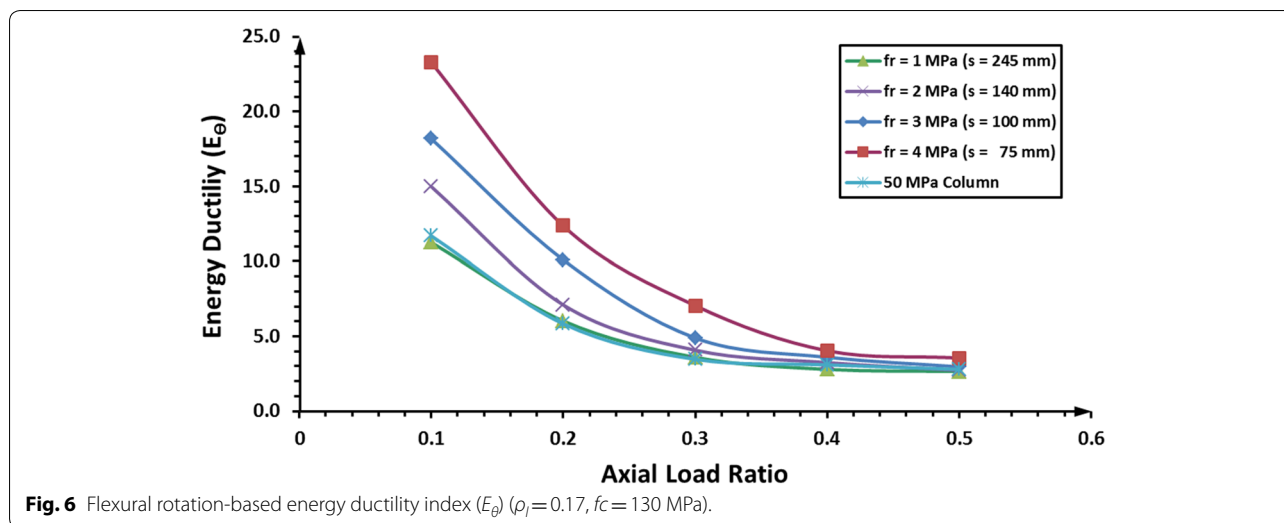
where L_p is the plastic hinge length and ϕ_y is yield curvature. The method proposed by Park et al. (1982) for plastic hinge lengths of HSC columns is used to calculate the plastic hinge length of VHSC columns. The yield rotation is defined as the rotation related to the yield curvature (ϕ_y). The ultimate rotation for the index is taken as the rotation at 0.8 times the peak moment at the post-peak branch. Thus, the index has a provision for sustaining the load carrying capacity beyond the peak moment.

Therefore, the new index gives better insight for ductility by considering energy dissipation characteristics, as well as the ability of VHSC columns to deform while sustaining its load carrying capacity. In order to calculate the rotational energy due to flexural rotation, rotation due to bond slip and shear deformation were not included in the calculation.

Figure 6 indicates the flexural rotation-based energy ductility (E_{θ}) for the column illustrated in Fig. 3a, with a compressive strength of 130 MPa, an axial load ratio varying from 0.1 to 0.5, a height of 3.3 m and confinement pressures in the range of 1 MPa to 4 MPa. The energy ductility values are higher than the curvature ductility for columns. Similarly, the curvature and energy ductility of columns with different geometries, compressive strengths, steel ratios and axial load levels can be evaluated using the analytical program. Subsequently, using a regression analysis on different parameters, the relationship between ductility and governing parameters can be established.

3.4 Validation of the Analytical Program Using Experimental Results for VHSC Columns

The flexural behaviour of HSC and VHSC columns has been studied by many researchers (Ho 2012; Li et al. 1991; Paultre et al. 2001; Saatcioglu and Razvi 1998). However, experimental results for VHSC columns are scarce in the literature. Experimental programs for columns with compressive strengths of around 100 MPa or more were conducted by (Azizinamini et al. 1994; Bayrak and Sheikh 1998; Paultre et al. 2001; Paultre and Légeron (2008)) and the results are given in Table 3. Figure 7 shows the comparison between analytical and experimental moment–curvature behavior. The secondary moment due to P– Δ effect at testing conditions is considered to calculate total moment.



Paultre and Légeron (2008) developed ductility guidelines using moment curvature analysis which is used by the CSA 23.3 (Canadian Code). The method used curvature ductility of experimental programs to validate the analytical program [Fig. 13 of Paultre and Légeron (2008)]. Similarly, Kwan and Ho (2010) used the same methodology for validating the analytical program and develop ductility design guidelines. Figure 8 shows a comparison between the theoretical curvature ductility and the experimental curvature ductility values. The developed stress-strain model for confined VHSC is not valid for confinements where the residual stress (f_{res}) is greater than the confined peak strength (f_{cc}). Thus, some of the columns that do not agree with the above criteria are omitted in the comparative study. The regression line is aligned with the $y=x$ line. The strong correlation between the theoretical prediction and the experimental results is indicated by a coefficient of correlation of $R^2=0.94$. Hence, the analytical method can sufficiently predict the curvature ductility of VHSC columns with strengths of around 100–110 MPa. Considering the validity of the stress-strain model up to 150 MPa, it is expected that the developed analytical program can predict the curvature ductility of concrete columns with a strength of up to 150 MPa with acceptable accuracy.

4 Method for Parametric Study and Developing Expressions for Ductility

According to the parametric study using analytical programs and as confirmed by many researchers, ductility is mainly governed by the axial load ratio, confinement pressure, compressive strength of concrete, section area ration and longitudinal steel ratio. Axial load ratio

affects the failure of concrete and steel. Accordingly, it affects the ductility dependent on material ductility of failing material. Confinement pressure provides hoop stress and constrain shear failure plane of the concrete. Thus, increase material ductility of post-peak branch of concrete which subsequently increases the ductility of column. Section area ratio which related to cover area of the column indicate the spalling of VHSC. Sudden reduction in the area due to spalling affects the moment-curvature behaviour of the column. In addition, longitudinal steel act as dowels for shear failure plan of concrete and increase the ductility.

Researchers (Bai and Au 2013; Kwan and Ho 2010; Mendis et al. 2000; Paultre and Légeron (2008)) developed analytical equations and design charts including these parameters. In this study, equations and parameters are proposed similar to the form of the equation suggested by Watson et al. (1994) because the equation consider the major parameters affect the ductility. The equation suggests four dimensionless parameters with different coefficients as outlined below.

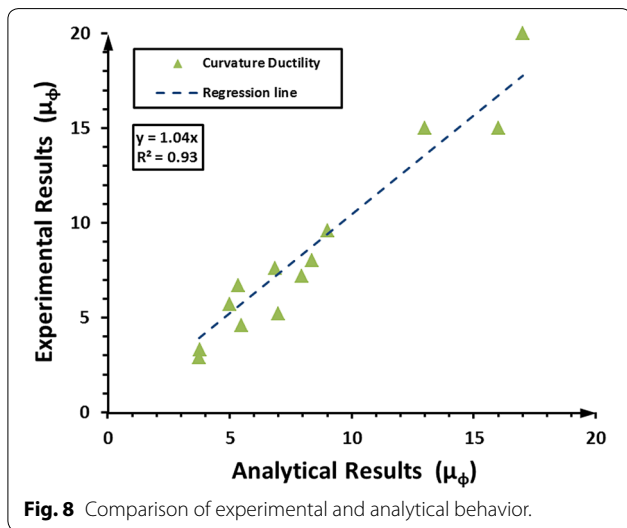
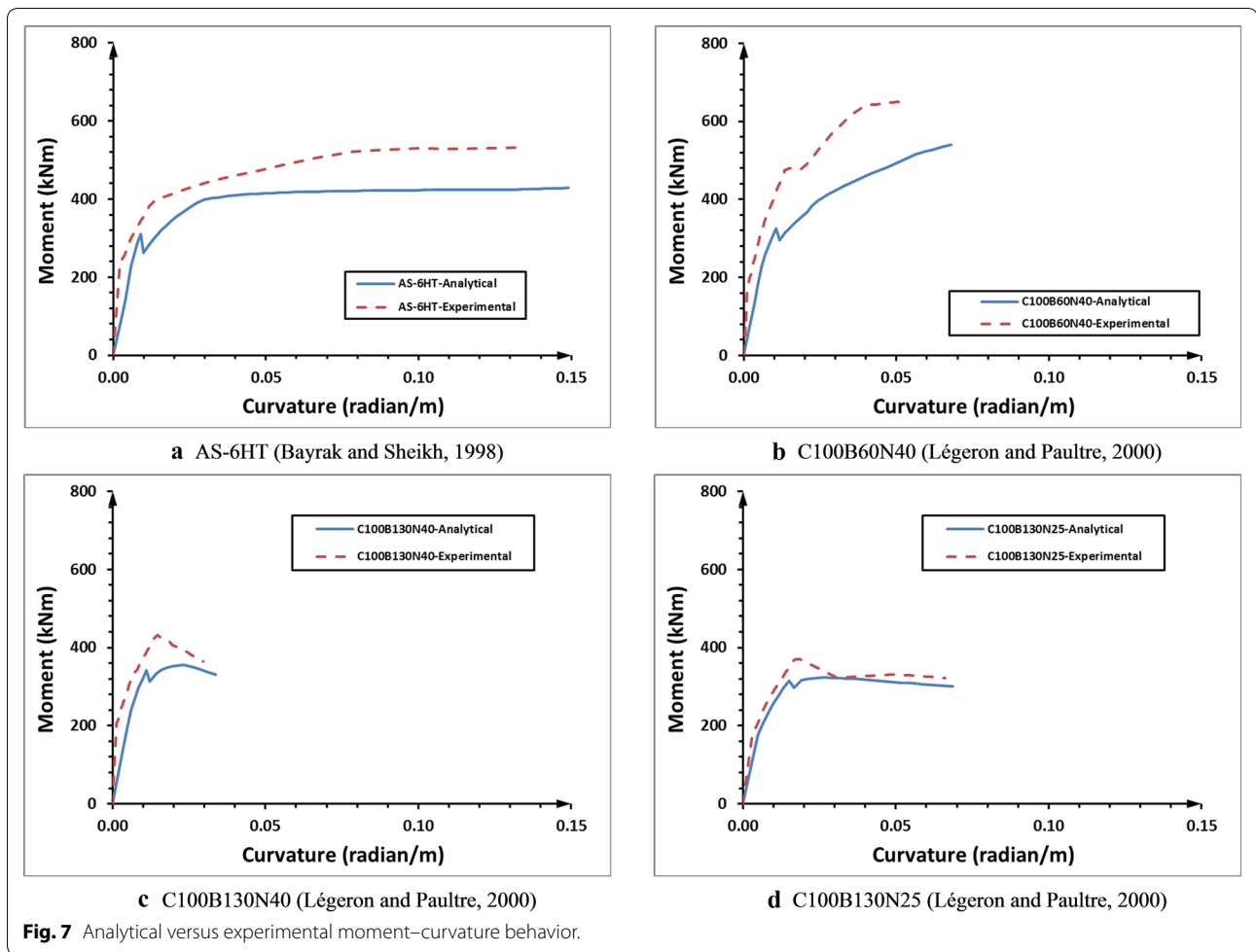
4.1 Governing Parameters

4.1.1 Axial Load Level Ratio ($P/A_g f_c$)

Axial load level ratio is the ratio of the applied axial load (P) to the axial compression capacity of the column ($A_g f_c$). The full axial compression capacity is calculated by taking the product of the gross cross-sectional area (A_g) and the compressive strength of concrete (f_c). The contribution to the load carrying capacity from the longitudinal steel is neglected. This factor represents the effect of axial load level on the ductility of columns.

Table 3 Experimental results for curvature ductility of VHSC columns.

Sample name	s (mm)	ρ_{st} (%)	f_t (MPa)	$P/A_s f_c$	f_c (MPa)	b (mm)	d (mm)	Cover (mm)	d_l (mm)	d_h (mm)	f_{syh} (MPa)	f_{syt} (MPa)	ϵ_s	ϵ_u	ϵ_{uh}	k_e	A_d (mm ²)	ρ_d	$H_{p,exp}$	$H_{p,ana}$	
Aziznamini et al. (1994)																					
D60-15-4	67	2.7	3.9	0.19	101	300	300	15.6	20	12.7	413	413	0.015	0.02	0.2	0.69	2389	0.027	15	13	
D120-15-3B	67	2.4	5.8	0.19	101	300	300	15.6	20	9.5	752	413	0.015	0.02	0.14	0.66	2389	0.027	20	17	
D120-15-3C	41	3.8	10.5	0.19	101	300	300	15.6	20	9.5	752	413	0.015	0.02	0.14	0.73	2389	0.027	20	-	
D60-15-3A	41	3.8	5.8	0.28	100	300	300	15.6	20	9.5	413	413	0.015	0.02	0.2	0.73	2389	0.027	15	16	
Bayrak and Sheikh (1998)																					
AS-7HT	94	2.72	4.5	0.45	102	305	305	15.6	20	11.3	542	454	0.015	0.13	0.155	0.61	2400	0.026	7.2	8.0	
AS-5HT	90	4.8	7.1	0.45	102	305	305	15.6	20	11.3/16	542	454	0.015	0.13	0.155	0.62	2400	0.026	9.6	9.0	
AS-6HT	76	6.74	10.6	0.46	102	305	305	15.6	20	16.0	463	454	0.015	0.13	0.113	0.68	2400	0.026	14	11.5	
ES-8HT	70	4.29	6.9	0.47	102	305	305	15.6	20	16.0	463	454	0.015	0.13	0.113	0.69	2400	0.026	6.7	5.3	
Légeron and Paultre (2000), Paultre et al. (2001)																					
C100BH55N40	55	3.30	9.6	0.35	110	305	305	12.5	20\16	9.5	825	450	0.007	0.11	0.065	0.71	2000	0.021	8	8.4	
C100B130N40	130	1.96	2.1	0.37	104	305	305	12.5	20\16	11.3	418	450	0.007	0.11	0.136	0.52	2000	0.021	2.9	3.8	
C100BH80N40	80	2.27	6.0	0.37	104	305	305	12.5	20\16	9.5	825	450	0.007	0.11	0.065	0.64	2000	0.021	4.6	5.5	
C100B60N40	60	4.26	6.3	0.39	98	305	305	12.5	20\16	11.3	418	450	0.007	0.11	0.136	0.70	2000	0.021	7.6	6.9	
C120B60N40	60	4.26	6.6	0.41	109	305	305	12.5	20\16	11.3	438	450	0.007	0.11	0.136	0.70	2000	0.021	5.2	7.0	
C100B60N52	60	4.26	7.4	0.51	109	305	305	12.5	20\16	11.3	492	450	0.007	0.11	0.136	0.70	2000	0.021	5.7	5.0	
Paultre and Légeron (2008)																					
C100B130N25	130	1.96	2.0	0.24	97.7	305	305	12.5	20\16	11.3	391	475	0.007	0.11	0.136	0.52	2000	0.021	3.3	3.8	



4.1.2 Confinement Pressure (f_r)

Confinement pressure represents the amount of confinement given to the core. In addition, it represents the transverse steel requirement (ρ_s) to obtain a particular curvature ductility. In this dimensionless parameter, the volumetric ratio and effective transverse steel strength is included, which improve the ductility due to confinement effects and the dowelling action of transverse steel against relative sliding of the failure planes. The confinement pressure is calculated using the method proposed by Mander et al. (1988).

4.1.3 Section Area Ratio (A_g/A_c)

This ratio represents the effect of early spalling of cover concrete. The section area ratio is given by the ratio of the gross area (A_g) to the core area (A_c).

4.1.4 Longitudinal Steel Ratio ($\rho_s f_{ysl}/f_c$)

Even though many researchers have not considered the effects of longitudinal steel, the experimental results showed that longitudinal steel improves the descending branch of core concrete due to dowelling action and constrains the movement of concrete. Thus, the material ductility of the confined core is enhanced, which results in improved column ductility. The dowelling action is related to the longitudinal steel ratio (ρ_s), compressive strength of concrete (f_c) and yield strength of longitudinal steel (f_y). In addition, the longitudinal steel ratio relates to the confinement effectiveness coefficient so that it is related to confinement pressure.

4.2 Proposed Expression for Curvature-Based Ductility Design

The following equation format, Watson et al. (1994) is proposed to develop mathematical expressions for curvature ductility:

$$\mu_\phi = k_1 \left(\frac{A_g}{A_c}\right)^{\alpha 1} \left(k_2 \frac{\rho_s f_{ysl}}{f_c} + k_3 \left(\frac{f_r}{f_c}\right) + k_4\right) \left(\frac{P}{A_g f_c}\right)^{\alpha 2} \left(\frac{f_{ysh}}{f_c}\right)^{\alpha 3} \tag{11}$$

where k_1 to k_4 are unknown coefficients, and $\alpha 1$ to $\alpha 3$ are indices that will be determined by regression analysis. Dimensionless parameters are used to establish the non-linear relationship between curvature ductility. The equation can be further simplified into the following formats once the coefficients are known from regression analysis:

$$f_r = \frac{f_c}{k_3} \left[\frac{\mu_\phi}{k_1} \left(\frac{A_g}{A_c}\right)^{\beta 1} \left(\frac{P}{A_g f_c}\right)^{\beta 2} \left(\frac{f_{ysh}}{f_c}\right)^{\beta 3} - \left(k_2 \frac{\rho_s f_{ysl}}{f_c} + k_4\right) \right] \tag{12}$$

where $\beta 1$ to $\beta 3$ are new coefficients. Using Eq. (12), the required confinement level to achieve a given curvature ductility can be calculated. The required confinement level can be determined by selecting a suitable transverse reinforcement arrangement and spacing using the method proposed by Mander et al. (1988).

Around 3200 rectangular columns with different section sizes and ranges of parameters, as shown in Table 4, are considered in the analytical study, and curvature ductility is evaluated from the full-range moment–curvature curves. Nonlinear regression analysis for the predicted ductility and dimensionless parameters is carried out to derive the prescribed mathematical expression.

The regression analysis gives a coefficient of determination R^2 of 0.85. Thus, the analytical data fits the statistic model well. The root mean squared error is low relative to the maximum and minimum values of the dependent

Table 4 Range of parameters for regression analysis.

Parameter	Unit	Range
Column size		
B	mm	500–2000
D	mm	500–2000
f_r	MPa	1–4 MPa
ρ_{sl}	–	1–4%
f_c	MPa	100–150 MPa
A_g/A_c	–	0.96–0.99
$P/A_g f_c$	–	0.1–0.5
f_{ysl}	MPa	250–500
f_{ysh}	MPa	250–800

variable; 18.9 and 2.5, respectively. P -values of the regression analysis for the coefficients are zero. Therefore, the null hypothesis, which is that the parameters do not relate to the dependent variable, can be neglected. This means that the parameters considered in the analysis are likely to be meaningful and have a relationship to the dependent variable. P -value analysis supports that parameters established from the parametric study have an effect on the ductility of VHSC columns.

The regression analysis gives Eq. (13) with the following coefficients and indices.

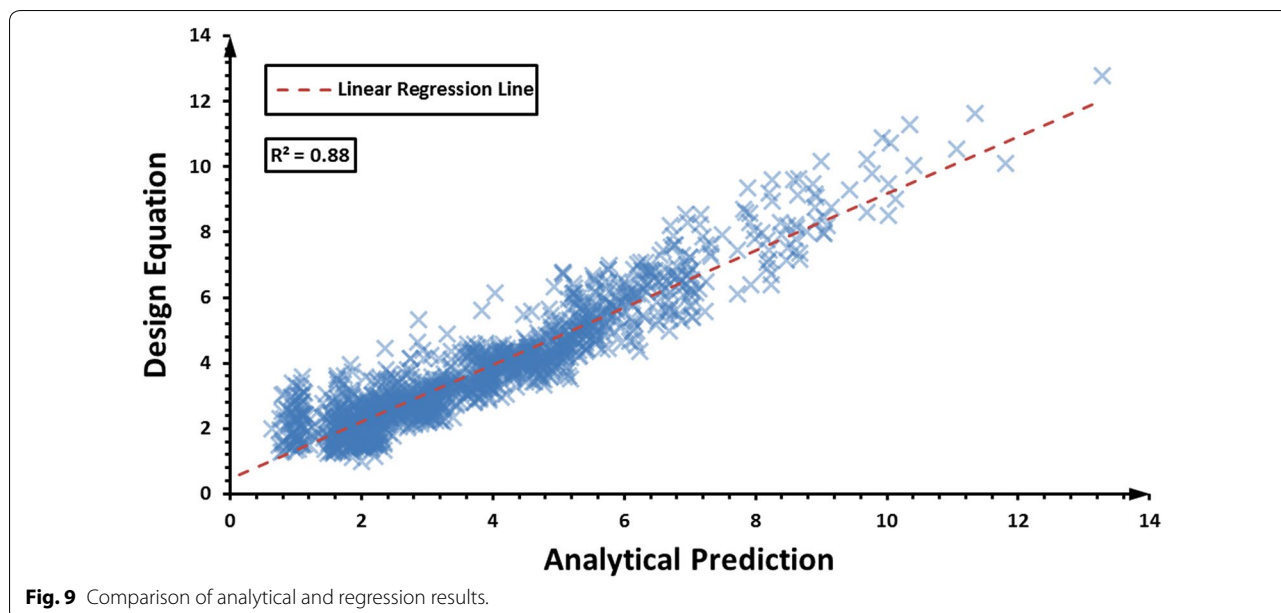
$$\mu_\phi = 3.64 \left(\frac{A_g}{A_c}\right) \left(2.9 \frac{\rho_s f_{ysl}}{f_c} + 26 \left(\frac{f_r}{f_c}\right)\right) \left(\frac{P}{A_g f_c}\right)^{-0.7} \left(\frac{f_{ysh}}{f_c}\right)^{-0.5} \tag{13}$$

The equation can be further simplified into the following expression in order to find the required confinement for given ductility demand:

$$f_r = \frac{f_c}{26} \left[\frac{1}{3.64} \mu_\phi \left(\frac{A_c}{A_g}\right) \left(\frac{P}{A_g f_c}\right)^{0.7} \left(\frac{f_{ysh}}{f_c}\right)^{0.5} - 2.9 \frac{\rho_s f_{ysl}}{f_c} \right] \tag{14}$$

Figure 9 shows the comparison between Eq. (13) and the analytical predictions. It can be concluded that the new expression given by Eq. (13) has a very good correlation with the analytical results. Thus, Eq. (14) can be used to find the required confinement level for the required ductility level. Since the equation targets the confinement pressure instead of the volumetric ratio of transverse steel, the proposed equation can be used for both circular and rectangular columns.

The regression equation has 50% probability of overestimation or underestimation. Though economically unacceptable, overestimation can be accepted because it results in higher ductility. However, underestimation



can cause severe failure in the structure during an earthquake event. Thus, the design equation should limit the probability of underestimation to an acceptable range. Therefore, the design equation should comply with a 95% confidence limit philosophy so that only 5% underestimation is possible. The following linear equation is proposed to satisfy the 95th percentile concept:

$$y = mx + c \tag{15}$$

Using this method, Eq. (16) with 95% confidence is derived for designing confinement for ductility:

$$f_r = \frac{f_c}{26} \left[\frac{1}{3.64} \mu_\phi \left(\frac{A_g}{A_c} \right) \left(\frac{P}{A_g f_c} \right)^{0.7} \left(\frac{f_{syh}}{f_c} \right)^{0.5} - 2.9 \frac{\rho_{st} f_{ysl}}{f_c} + 0.0065 \right] \geq 0 \tag{16}$$

Once the required curvature ductility level is known, the structural members can be designed for anticipated curvature ductility using Eq. (16). Figures 10 and 11 show the steel confinement requirements for different ductility levels, $\mu_\phi=4$ and 6 for typical 1500 × 1500 mm VHSC columns with compressive strengths in the range of 100 to 150 MPa; axial load ratios of 0.1, 0.3 and 0.5; and longitudinal ratios of 2.0 and 4.0% with 500 MPa transverse and longitudinal steel reinforcement. The first and second columns compared the required volumetric ratio and spacing of transverse steel to the compressive strength of concrete, respectively. Generally, very low confinement levels are given for lower axial load levels and lower longitudinal steel ratios because steel yields prior to the crushing of concrete. Therefore, it must be

noted that if the confinement requirement for ductility is less than the transverse reinforcement requirement to prevent buckling and spalling, then transverse steel reinforcement design is governed by the anti-buckling or spalling requirement.

The analysis shows that the required confinement levels to gain curvature ductility of 4 and 6 are very high for higher axial load levels and higher strengths. Therefore, a large amount of transverse steel is required. However, providing a transverse steel ratio of more than 4% causes congestion in the reinforcement and is not practical (Paultre et al. 2001). The spacing to gain the above curvature ductility levels is very low and difficult for construction. Therefore, gaining such ductility is not practical using normal yield strength steel (less than 500 MPa). Therefore, using high yield strength steel (greater than 500 MPa) can be an alternative to gaining a higher confinement pressure whilst increasing the spacing and reducing the transverse steel ratio. Curvature ductility levels of 10 and 16 are proposed by CSA (2004) for moderate ductile and ductile structures, respectively. NZS 3101.1 (2006) proposes curvature ductility levels of 11 and 19 for nominal ductile and ductile structures/hinges, respectively. However, the study implied that even using very-high yield strength steel is onerous to gain such high ductility levels at higher axial load levels.

4.3 Limited Ductility Design of VHSC Columns

4.3.1 Proposed Expression for Curvature-Based Nominal Ductility Design of VHSC Columns

Based on studies by Foster (1999), the limited ductile design in AS 3600 (2009) suggests that the ductility level of a 50 MPa column detailed according to the minimum

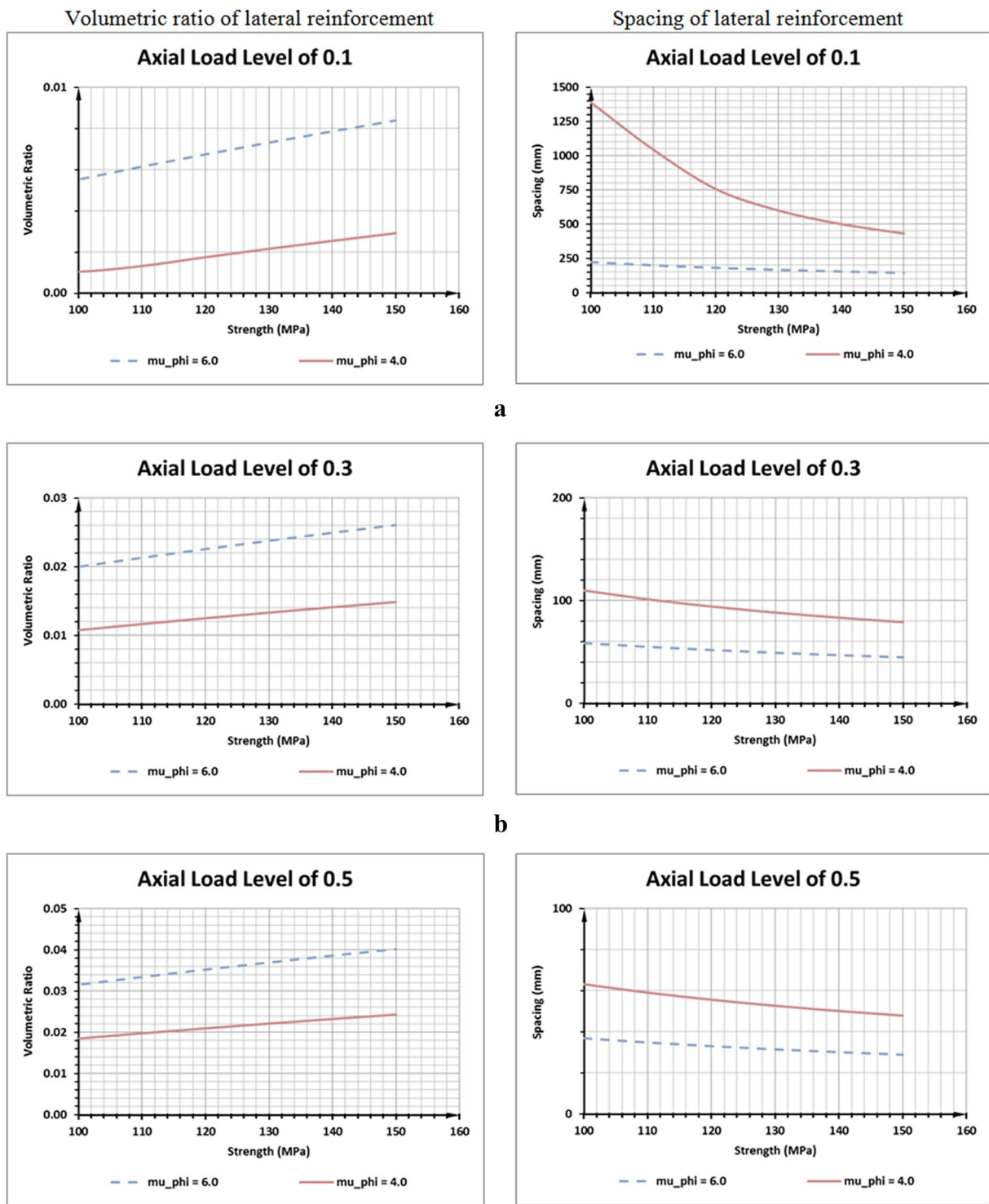
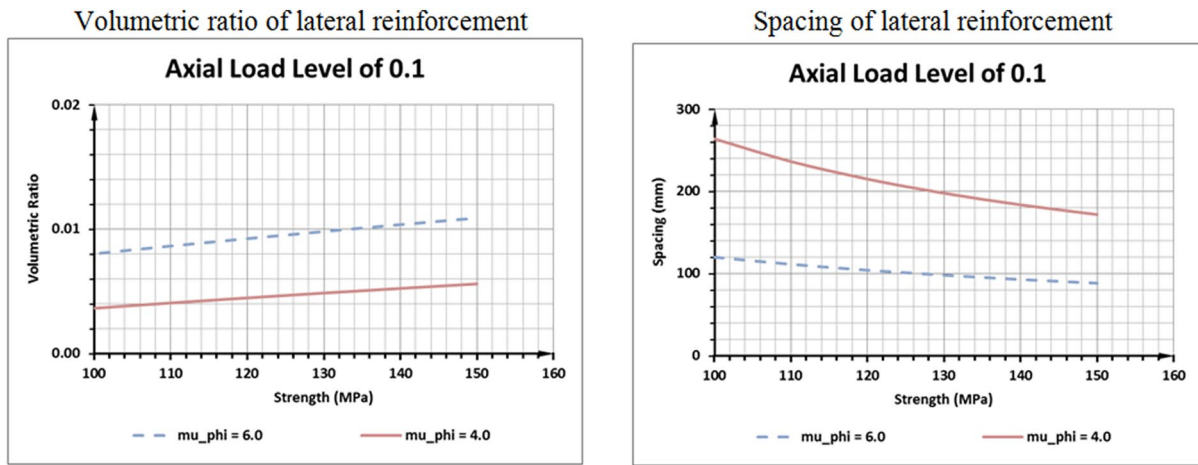
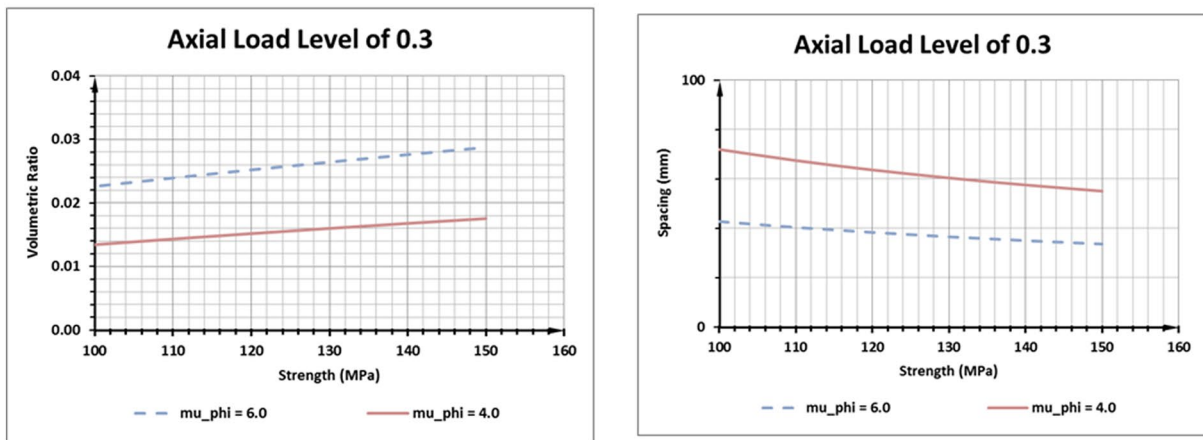


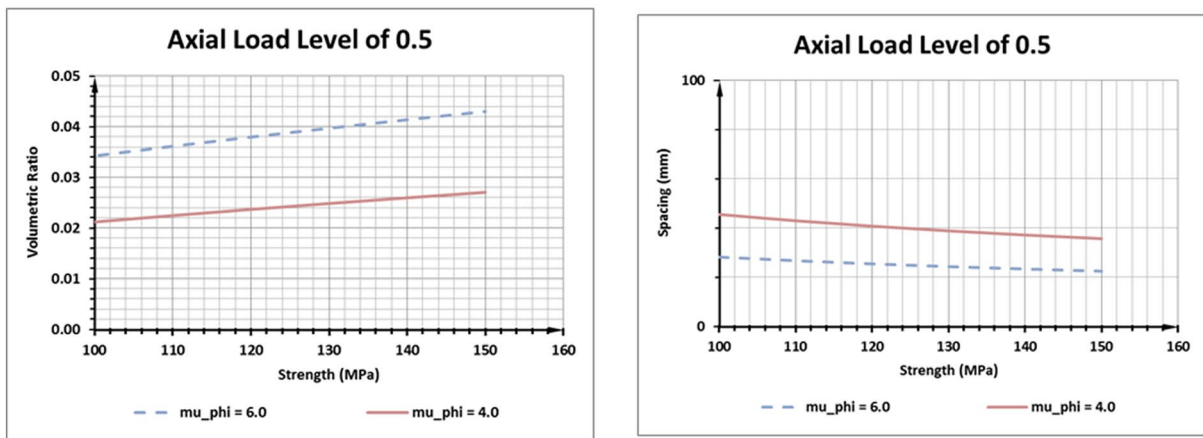
Fig. 10 Required volumetric ratio of transverse steel for different ductility levels ($\mu_\phi = 4$ and 6) ($\rho_{sl} = 4.0\%$) 1500×1500 mm, $f_{ysh} = f_{ysl} = 500$ MPa: **a** $P/f_{cc}A_c = 0.1$, **b** $P/f_{cc}A_c = 0.3$, **c** $P/f_{cc}A_c = 0.5$.



a



b



c

Fig. 11 Required volumetric ratio of transverse steel for different ductility levels ($\mu_\phi = 4$ and 6) ($\rho_{sl} = 2.5\%$) 1500×1500 mm, $f_{ysh} = f_{ysl} = 500$ MPa: **a** $P/f_{cc}A_c = 0.1$, **b** $P/f_{cc}A_c = 0.3$, **c** $P/f_{cc}A_c = 0.5$.

requirements of AS 3600 (2009) is adequate for ordinary moment resisting structures. This is due to the fact that an equivalent 50 MPa column has adequate ductility and the code does not specify any additional confinement to achieve ductility. In this study, a similar approach is suggested for nominal ductility design with low-seismic demands. The basis for curvature-based nominal ductility design is to provide similar curvature ductility to a 50 MPa column with equivalent geometry and axial load level, detailed according to the minimum requirements specified in AS 3600 (2009). Thus, the required nominal ductility levels of Eq. (16) shall be similar to the curvature ductility level of an equivalent 50 MPa column. Using the analytical program, the curvature ductility of 50 MPa rectangular columns with different geometries and detailed according to the minimum requirements of AS 3600 (2009) is evaluated at different axial load levels; for a 50 MPa concrete column, the stress-strain behaviour of confined and unconfined concrete proposed by Mendis et al. (2000) is used in the analytical study. The columns with compressive strengths of 50 MPa used in the present study have different ductility levels which depend on the axial load level. Thus, the required nominal ductility levels in Eq. (16) for VHSC columns must be modified according to the different axial load levels of a 50 MPa column. The expression given by Eq. (17) is derived using regression analysis for the ductility of a 50 MPa column with different axial load levels. Thus, Eq. (17) is proposed for determining the nominal curvature ductility level of VHSC columns with different axial load levels.

$$\mu_{\phi,nominal} = 1.757 \left(\frac{P}{A_g f_c} \right)^{-0.4} \tag{17}$$

Therefore, combining Eqs. (16) and (17), the following equation can be derived for the minimum ductile design of VHSC columns:

$$f_r = \frac{f_c}{26} \left[0.676 \left(\frac{A_g}{A_c} \right) \left(\frac{P}{A_g f_c} \right)^{0.3} \left(\frac{f_{syh}}{f_c} \right)^{0.5} - 2.9 \frac{\rho_s f_{ysl}}{f_c} + 0.0065 \right] \geq 0 \tag{18}$$

For lower axial load levels and lower longitudinal steel ratios, steel yields prior to the crushing of concrete and can sustain large deformation. Therefore, columns subject to the above criteria have higher curvature ductility levels. Thus, the required confinement level to achieve nominal ductility is less, and the equation may give negative or very low confinements for nominal ductility. As such, the transverse requirement for anti-buckling or spalling must be set as the minimum transverse reinforcement.

4.3.2 Proposed Expression for Energy-Based Nominal Ductility Design

As discussed previously, considering the drawbacks of curvature ductility in capturing the enhanced plastic energy of VHSC columns at higher axial load levels and higher strengths, this study suggests that the flexural rotation-based energy ductility ($E_{\theta-}$) as the ductility index, and the ductility level of an equivalent 50 MPa column with similar geometry and axial load levels as the nominal ductility level of VHSC columns, considering the fact that a 50 MPa column has adequate ductility for limited ductility demands; This is somewhat similar to the approach of AS (2009) which proposed by Foster (1999).

A parametric study showed that axial load ratio, confinement pressure, compressive strength, cover and longitudinal reinforcement ratio have effects on flexural rotation-based ductility index, E_{θ} . An equation format that is similar to Eq. (11) with similar dimensionless parameters is used in the regression analysis, considering the similarity of parameters for the curvature ductility index and energy ductility index. The energy ductility index is calculated for the range of parameters given in Table 4. Nonlinear regression analysis, similar to the previous analysis, is carried out for the prescribed equation and analytical results. Excluding the outliers, regression analysis is carried out for a better statistical fit of the analytical data. The regression analysis gives Eq. (19), with the following coefficients and indices, and the equation has a very good agreement with the analytical results. Once the outliers are removed, the coefficient of correlation of the proposed equation is 0.90, which is acceptable to predict the flexural rotation-based energy ductility (E_{θ}) of VHSC columns.

$$E_{\theta} = 5.04 \left(\frac{A_c}{A_g} \right) \left(3.33 \frac{\rho_s f_{ysl}}{f_c} + 35 \left(\frac{f_r}{f_c} \right) \right) \left(\frac{P}{A_g f_c} \right)^{-0.7} \left(\frac{f_{syh}}{f_c} \right)^{-0.5} \tag{19}$$

The equation can be further simplified into the following equation to find the required confinement level:

$$f_r = \frac{f_c}{35} \left[\frac{1}{5.04} E_{\theta} \left(\frac{A_g}{A_c} \right) \left(\frac{P}{A_g f_c} \right)^{0.7} \left(\frac{f_{syh}}{f_c} \right)^{0.5} - 3.33 \frac{\rho_s f_{ysl}}{f_c} \right] \tag{20}$$

Figure 12 shows a comparison between the design equation and analytical predictions. It can be concluded that the new expression given by Eq. (19) has a very good correlation with the analytical results. Thus, Eq. (20) can be used to find the required confinement level for a particular energy ductility level. Since the equation is

developed to target the confinement pressure instead of the volumetric ratio of transverse steel, the equation can be used for both circular and rectangular columns.

The following equation, which satisfies the 95th percentile, can be proposed for the confinement pressure versus the energy ductility index. Thus, Eq. (21) can be used to determine the required confinement level for energy-based nominal ductility design.

$$f_r = \frac{f_c}{35} \left[\frac{1}{5.04} E_\theta \left(\frac{A_g}{A_c} \right) \left(\frac{P}{A_g f_c} \right)^{0.7} \left(\frac{f_c}{f_{ysh}} \right)^{0.5} - 3.33 \frac{\rho_s f_{ysl}}{f_c} + 0.0076 \right] \tag{21}$$

The energy ductility of 50 MPa columns detailed according to the minimum requirements of AS 3600 (2009) is suggested for nominal ductility design. Using regression analysis, the expression given by Eq. (22) is proposed for the energy ductility levels of 50 MPa columns, with the minimum detailing requirements specified in AS 3600 (2009). Thus, the nominal energy ductility level of VHSC columns is given by Eq. (22) for different axial load levels.

$$E_{\theta, nominal} = 2.12 \left(\frac{P}{A_g f_c} \right)^{-0.4} \tag{22}$$

Combining and simplifying Eqs. (21) and (22), the required transverse steel quantity can be found for energy-based nominal ductile design, which is represented by the following expression:

$$f_r = \frac{f_c}{35} \left[0.42 \left(\frac{A_g}{A_c} \right) \left(\frac{P}{A_g f_c} \right)^{0.3} \left(\frac{f_{ysh}}{f_c} \right)^{0.5} - 3.33 \frac{\rho_s f_{ysl}}{f_c} + 0.0076 \right] \tag{23}$$

4.3.3 Comparison Between the Proposed and Existing Confinement Design Equations

The curvature-based method and energy-based method for nominal ductility design are compared with the existing expression proposed by CSA (2004), ACI 318 (2011) and EC 8 (2004a). However, it must be noted that these methods are not applicable or developed for strengths up to 150 MPa, and the results have been extended/extrapolated for strengths up to 150 MPa though it is not appropriate. The strength limits of guidelines and codes are given in Tables 1 and 2. The results are extended over the material strengths limits of codes and guidelines just to give an indication on confinement requirement of the new methods if strength limits can be extrapolated. For nominal ductility levels, NZS 3101.1 (2006) specified a 70% transverse reinforcement requirement of ductile design (with $\mu_\phi=19$) due to anticipated higher seismic demands in the region, and regions with low-seismic demands may not require much ductility. Thus, NZS 3101.1 (2006) gives a large amount of transverse steel for nominal ductility design. Unrealistic volumetric ratios that cannot practically be provided for columns are given by NZS 3101.1 (2006). Therefore, NZS 3101.1 (2006) is excluded in the following comparison.

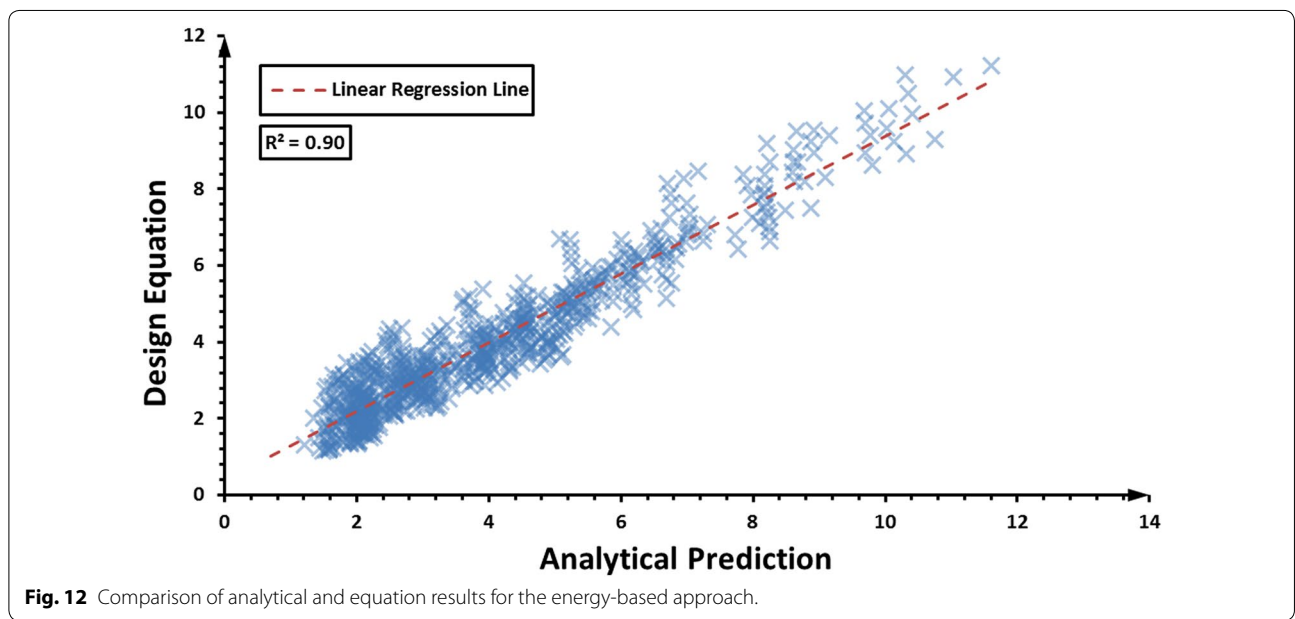


Fig. 12 Comparison of analytical and equation results for the energy-based approach.

Figures 13, 14, and 15 compare the transverse steel requirements for a typical nominal ductile VHSC column with a square cross-section of 1500×1500 mm, compressive strengths of 100 to 150 MPa, axial load levels of 0.1, 0.3 and 0.5, and longitudinal ratios of 1.0%, 2.5% and 4.0%, with 500 MPa transverse and longitudinal steel. The first and second columns of graphs show the variations in the required volumetric ratio and spacing of transverse steel with the compressive strength of concrete, respectively. As mentioned previously, for lower axial load ratios, the required confinement level to gain nominal ductility is low and can be negative in some instances. Therefore, a minimum transverse steel amount is set to satisfy the requirement for anti-buckling as specified in AS 3600 (2009).

CSA 23.3 (2004) and EC 8 (2004a) standards do not give any guidelines for nominal ductility, and transverse steel requirements are governed by the anti-buckling condition. Thus, Constant volumetric ratios are given by these codes for nominal ductility design, regardless of different axial load levels, compressive strengths and longitudinal steel ratios: In order to calculate transverse steel requirement for anti-buckling, the diameter of longitudinal steel is considered as greater than or equal to 25 mm. AS 3600 (2009), which is based on an energy-based method (I_{10}), gives a volumetric ratio of transverse steel, considering the effects of axial load ratio and the compressive strength of concrete. The code has not included the effects from the dowelling action of longitudinal and transverse steel, although it considers the effects of steel configuration on the confinement pressure.

According to Figs. 13, 14, and 15, transverse steel requirements for curvature ductility-based design and energy-based design are increasing with the increase of strength and axial load levels. The material model used for confined VHSC considered the contribution of dowelling effects of longitudinal and transverse steel on the plastic behaviour of confined concrete. Thus, the longitudinal steel ratio has a contribution to the ductility of the material, and consequently, to the ductility of the column. The comparison between Figs. 13 and 15 showed that increasing the longitudinal steel ratio decreases the transverse steel quantity. The gap between curvature-based design and energy-based design is increasing with the increase of strength and axial load level. It can be concluded that the increment of transverse steel required for an increase of strength and axial load are not similar for curvature- and energy-based ductility design. The transverse steel requirement for curvature-based design is much higher than that for energy-based design when the strength of concrete and axial load levels increase. For higher compressive strengths and axial load levels, VHSC columns have higher peak moments relative to the yield

moments. Therefore, it results in higher plastic energy in the moment–curvature graph. Thus, energy ductility is relatively high, requiring a lower amount of transverse steel relative to curvature-based design. However, the enhancement in energy is not captured by the curvature ductility index and gives higher confinement relative to the energy-based method. Therefore, the energy-based approach provides an economical design for VHSC columns. The comparison shows that VHSC columns can obtain nominal energy and curvature ductility levels using practical stirrup spacing and can be used in structures located in low-seismic regions with nominal ductility demands.

5 Conclusion

The paper presents an algorithm to predict the ductility of VHSC columns using a novel confined concrete model that is valid up to 160 MPa. Approximately 3200 columns with different parameters were analysed using the analytical program proposed in the study. The parametric study and the literature review on ductile columns concluded that the following parameters govern the ductility of VHSC columns: (1) axial load ratio ($P/A_g f_c$), (2) confinement effectiveness factor ($\rho_f f_{ys}/f_c$), (3) section area ratio (A_g/A_c), and (4) longitudinal steel ratio ($\rho_f f_y/f_c$). Using the analytical results, new expressions are developed to predict curvature ductility and energy ductility of VHSC columns.

Considering the fact that VHSC columns have higher plastic energy at higher axial load levels and higher strengths, the flexural energy-based ductility index is proposed for the nominal ductility design for VHSC columns. Curvature ductility and flexural rotation-based energy ductility of an equivalent 50 MPa column with similar axial load levels detailed according to the minimum reinforcement requirements in AS 3600 (2009) are proposed as the nominal ductility level for curvature and energy-based design approaches, respectively. Theoretical expressions for the nominal ductility design of VHSC rectangular columns are developed using curvature ductility and the new energy-based ductility approach. Comparisons between the new methods for nominal ductility design and existing codes of practice showed that the new energy-based definition requires lower confinement levels with respect to the method based on curvature ductility.

Analysis on confinement requirements for different curvature ductility levels ($\mu_\phi = 4$ and 6) concluded that obtaining higher ductility levels is not practical for higher axial load levels using normal strength steel (less than 500 MPa) as the transverse steel. Therefore, the use of high yield strength steel (greater than 500 MPa) could

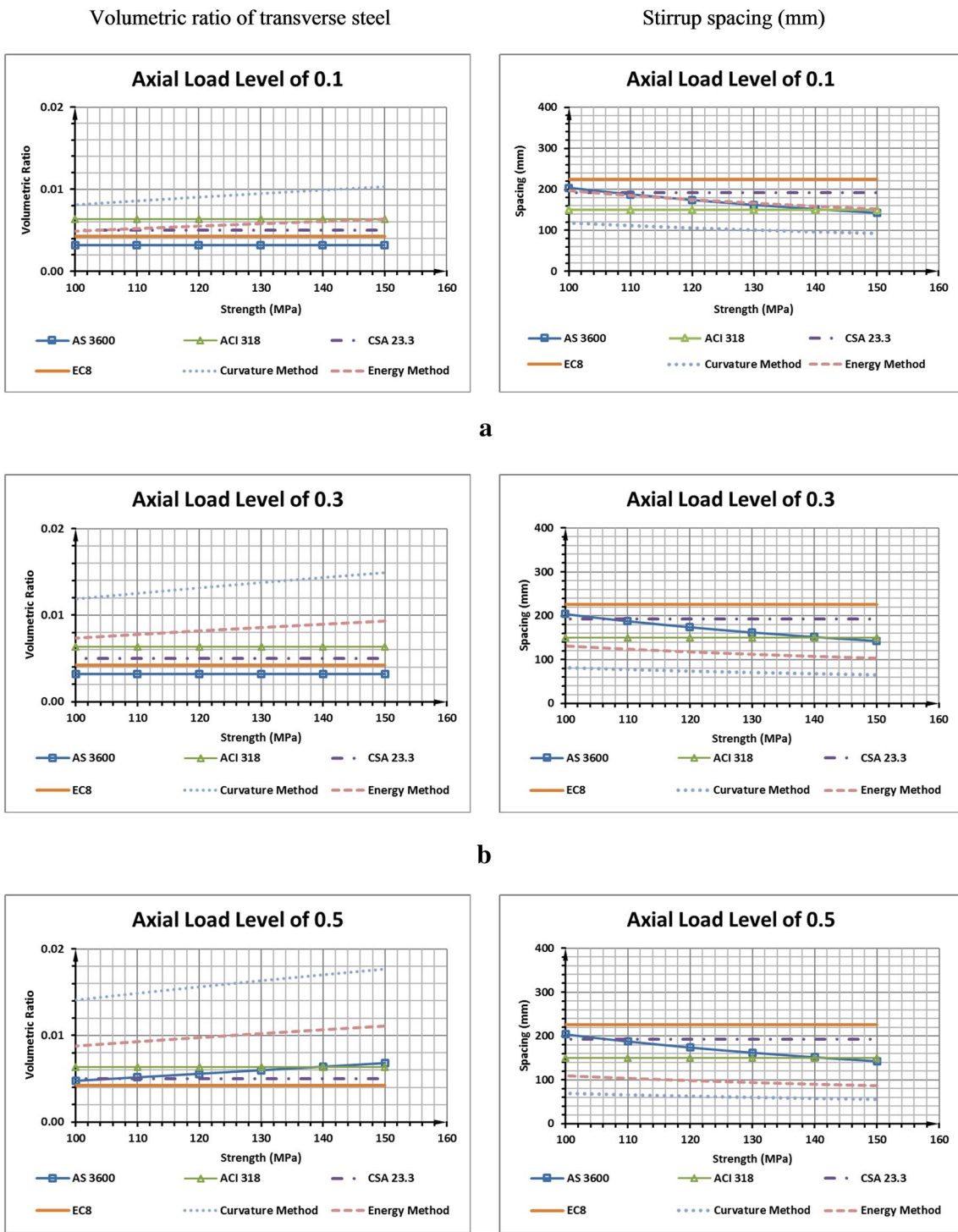


Fig. 13 Required volumetric ratio of transverse steel and stirrup spacing ($\rho_{st} = 1.0\%$) 1500×1500 mm, $f_{ysh} = f_{ysl} = 500$ MPa: **a** $P/f_{cc}A_c = 0.1$, **b** $P/f_{cc}A_c = 0.3$, **c** $P/f_{cc}A_c = 0.5$.

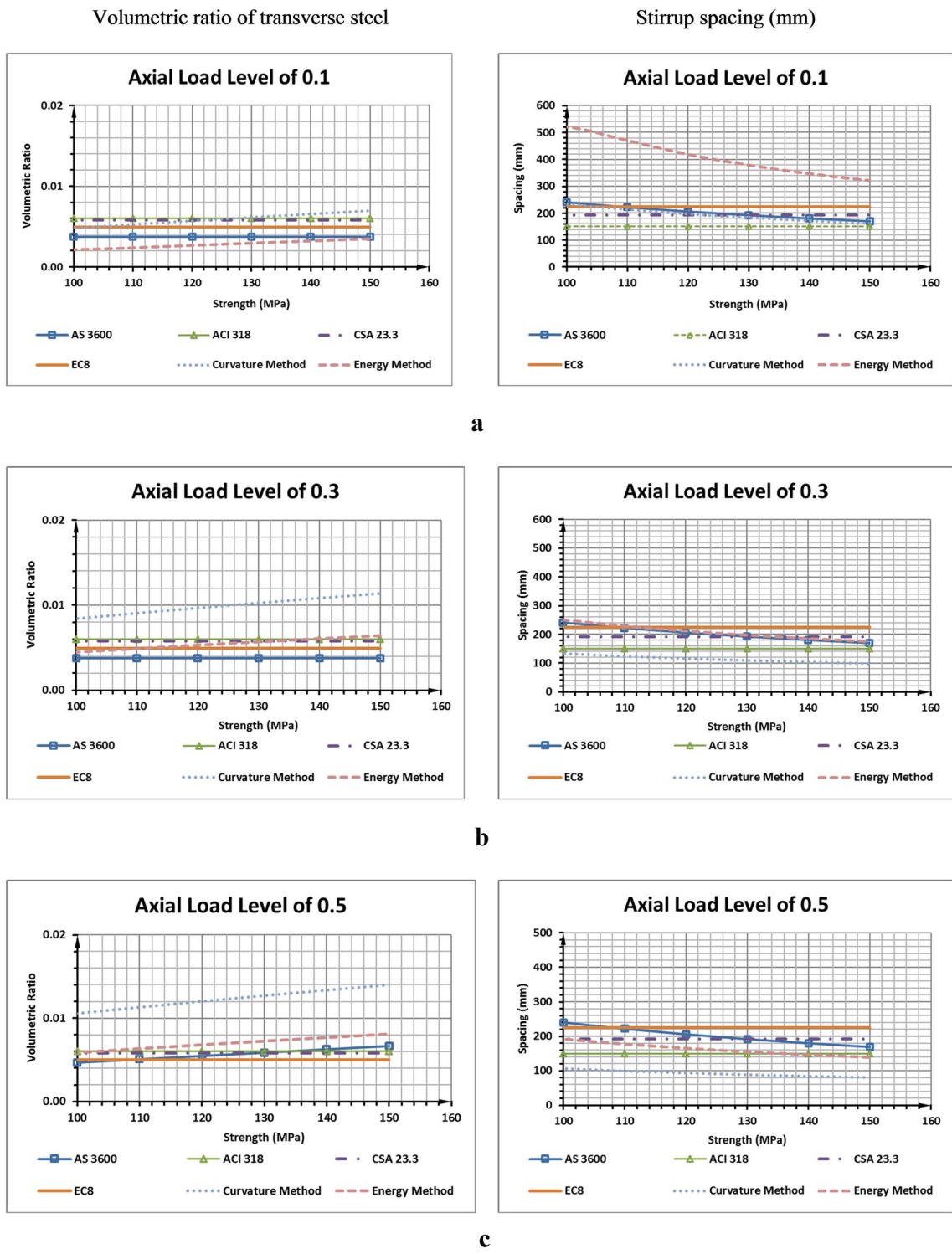
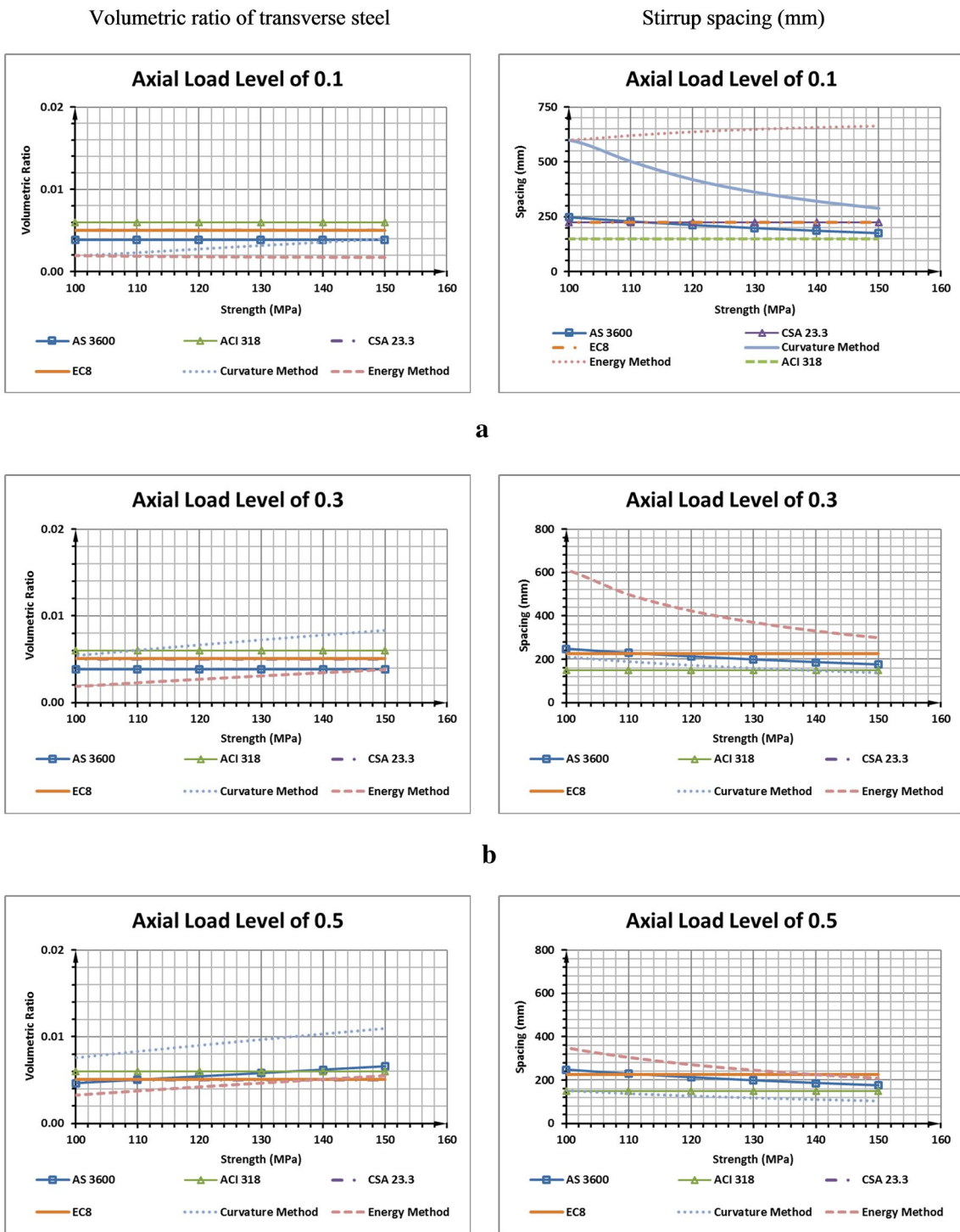


Fig. 14 Required volumetric ratio of transverse steel and stirrup spacing ($\rho_{st} = 2.5\%$) 1500×1500 mm, $f_{ysh} = f_{ysl} = 500$ MPa: **a** $P/f_{cc}A_c = 0.1$, **b** $P/f_{cc}A_c = 0.3$, **c** $P/f_{cc}A_c = 0.5$.



a

b

c

Fig. 15 Required volumetric ratio of transverse steel and stirrup spacing ($\rho_{st} = 4.0\%$) 1500×1500 mm, $f_{ysh} = f_{ysl} = 500$ MPa: **a** $P/f_{cc}A_c = 0.1$, **b** $P/f_{cc}A_c = 0.3$, **c** $P/f_{cc}A_c = 0.5$.

be an option to gain some moderate ductility. The analysis concludes that even if high yield transverse steel is used, it is onerous to provide the required volumetric ratios and spacings for higher ductility demands in moderate and high ductile structures. Therefore, VHSC columns in seismic regions, where columns can have plastic hinges with moderate ductile demands and high ductile demands, should be used with special care; and alternative passive techniques such as steel jacketing, fibre reinforced polymer (FRP) wraps, and steel/concrete composite columns should be considered as alternatives.

Using a new energy-based ductile design for VHSC columns with nominal ductility demands, where the structure or columns are subject to low-seismic events and the columns are specially designed with sufficient strength to provide a high degree of protection to avoid plastic hinging, ductility can be achieved using practical transverse steel ratios and spacings using normal yield strength steel. However, more experimental programs including columns with compressive strengths up to 150 MPa and subject to lateral loading are preferred by authors to further validate the analytical study and the new energy-based approach as a basis for the nominal ductility design of VHSC columns.

Abbreviations

A_c : core concrete area; A_g : gross concrete area; A_{sc} : area of compressive reinforcement; A_{st} : area of tensile reinforcement; b : breadth of the column; c_1 and c_2 : lengths of cover concrete; CDS: ductile structures; d_1 and d_2 : depth from the top of the column; d_c : depth of the centroid; DCH: ductility class high; DCL: ductility class low; DCM: ductility class medium; d_n : depth of the neutral axis; DS: ductile structure; DS: ductile structures; E_g : flexural rotation-based energy ductility index; f_c : compressive strength of concrete; f_{cc} : confined peak strength; f_r : confinement pressure; f_{res} : residual stress; f_y : yield strength of longitudinal steel; f_{ysh} : yield strength of lateral steel reinforcement; h : width of the column; HSC: high-strength concrete; I_{Dg} : energy-based ductility index; IMRF: intermediate moment resisting frames; LDS: limited ductile structures; M : moment capacity; MDS: moderate ductile structures; N : axial force; NDS: nominal ductile structures; OMRF: ordinary moment resisting frames; P : force; SMRF: special moment resisting frames; VHSC: very-high strength concrete; x : distance from the top to any arbitrary fiber of the section; ϵ_{ce} : compressive strain at the extreme compression fiber; ϵ_{tc} : compressive strain at the top reinforcement; ϵ_{st} : tensile strain at the bottom reinforcement; ϵ_{su} : ultimate strain of the lateral steel reinforcement; θ : rotation of the column; θ_{ϕ} : rotation at ϕ_u ; θ_y : yield rotation; μ_d : displacement ductility; μ_{ϕ} : curvature ductility; ρ_l : longitudinal steel ratio; ρ_v : volumetric ratio; ρ_s : transverse steel ratio; σ_{cc} : stress of confined concrete; σ_{cu} : stress of unconfined concrete; σ_{st} : stress of compression steel; σ_{st} : stress of tensile steel; ϕ : curvature at the extreme compression fiber; ϕ_u : ultimate curvature; ϕ_y : yield curvature.

Acknowledgements

The authors would like to thank Australian Research Council (ARC) for the Industrial Transformation Training Centres grant IC150100023 that has supported the authors to conduct the research.

Authors' contributions

KKB—Writing the manuscript and analytical program, analysing data, development of equations. PM—Developing the algorithm and excel files. Writing the manuscript. Literature review. TDN—Writing the manuscript. Analysing the data. Reviewing. MS—Writing the manuscript. Analysing the data. Reviewing. All authors read and approved the final manuscript.

Funding

Not applicable.

Availability of data and materials

Not applicable.

Ethics approval and consent to participate

Not applicable.

Consent for publication

Not applicable.

Competing interests

The authors declare that they have no competing interests.

Received: 2 May 2018 Accepted: 13 May 2019

Published online: 03 June 2019

References

- ACI 318. (2011). *Building code requirements for structural concrete (ACI 318-11) and commentary*. Farmington Hills, MI: American Concrete Institute.
- AS 3600. (2009). *AS 3600-Concrete structures*. Sydney: AS 3600.
- ASTM C 1018. (1992). *Standard test method for flexural toughness and first crack strength of fibre reinforced concrete (Using beam with third-point loading)*. Philadelphia, United States: American Society of Testing and Materials.
- Attard, M. M., & Setunge, S. (1996). Stress-strain relationship of confined and unconfined concrete. *ACI Materials Journal*, 93(5), 432–442.
- Azizinamini, A., Kuska, S. S. B., Brungardt, P., & Hatfield, E. (1994). Seismic behavior of square high-strength concrete columns. *ACI Structural Journal*, 91, 3.
- Bae, S. (2006). *Seismic performance of full-scale reinforced concrete columns* (Ph.D.). The University of Texas, United States. Retrieved from <http://search.proquest.com.ezp.lib.unimelb.edu.au/pqdtft/docview/304978434/abstract/13F4BC7288C6D78AA59/165?accountid=12372>.
- Bae, S., Mieses, A. M., & Bayrak, O. (2005). Inelastic buckling of reinforcing bars. *Journal of Structural Engineering*, 131(2), 314–321.
- Bai, Z. Z., & Au, F. T. K. (2013). Flexural ductility design of high-strength concrete columns. *The Structural Design of Tall and Special Buildings*, 22(1), 92–115. <https://doi.org/10.1002/tal.662>.
- Bayrak, O. (1995). *High strength concrete columns subjected to earthquake type loading (MAsc)*. Canada: University of Toronto.
- Bayrak, O., & Sheikh, S. (1998). Confinement Reinforcement Design Considerations for Ductile HSC Columns. *Journal of Structural Engineering*, 124(9), 999–1010. [https://doi.org/10.1061/\(ASCE\)0733-9445\(1998\)124:9\(999\)](https://doi.org/10.1061/(ASCE)0733-9445(1998)124:9(999)).
- Bayrak, O., & Sheikh, S. A. (2001). Plastic Hinge Analysis. *Journal of Structural Engineering*, 127(9), 1092.
- Bresler, B., & Gilbert, P. H. (1961). Tie requirements for reinforced concrete columns. *ACI Journal Proceedings* (Vol. 58). New York: ACI.
- Candappa, D. P., Setunge, S., & Sanjayan, J. G. (1999). Stress versus strain relationship of high strength concrete under high lateral confinement. *Cement and Concrete Research*, 29(12), 1977–1982.
- CSA 23.3. (2004). *Design of concrete structures CSA 23.3*. Mississauga, Ont: Canadian Standard Association.
- Cusson, D., & Paultre, P. (1995). Stress-strain model for confined high-strength concrete. *Journal of Structural Engineering*, 121(3), 468–477. [https://doi.org/10.1061/\(ASCE\)0733-9445\(1995\)121:3\(468\)](https://doi.org/10.1061/(ASCE)0733-9445(1995)121:3(468)).
- EC 2. (2004). *Design of concrete structures—Part 1*. European Union: Comité Européen de Normalisation.
- EC 8. (2004a). *Design of structures for earthquake resistance—Part 1: General rules, seismic actions and rules for buildings*. European Union: Comité Européen de Normalisation.
- EC 8. (2004b). *Eurocode 8: Design of structures for earthquake resistance—Part 1: General rules, seismic actions and rules for buildings*. European Union: Comité Européen de Normalisation.
- Elmshawi, A. A. A. (2008). *Ductility of ultra-high strength concrete flexural elements subjected to seismic shear* (Ph.D.). University of Calgary, Canada. Retrieved from <http://search.proquest.com.ezp.lib.unimelb.edu.au/pqdtft/docview/230868193/abstract/13EB5AF71A03BB0063C/3?accountid=12372>.

- Foster, S. J. (1999). *Design and detailing of high strength concrete columns*. Sydney: University of New South Wales, School of Civil Engineering.
- Foster, S. J., & Attard, M. M. (1997). Experimental tests on eccentrically loaded high strength concrete columns. *ACI Structural Journal*, 94(3). <http://www.concrete.org/publications/internationalconcreteabstractsportal.aspx?m=details&i=481>. Accessed 19 June 2015.
- Ho, J. C. M. (2012). Experimental tests on high-strength concrete columns subjected to combined medium axial load and flexure. *Advances in Structural Engineering*, 15(8), 1359–1374.
- Kristombu Baduge, S. (2016). *Ductility design of very-high strength reinforced concrete columns (100–150 MPa)*. Melbourne, Australia: The University of Melbourne.
- Kristombu Baduge, S., Mendis, P., Lee, L., Vanissorn, V., & Thilakarathne, P. S. (2018). Importance of selecting suitable coarse aggregate to produce very-high-strength concrete (> 100 MPa). In *Presented at the Australasian conference on the mechanics of structures and materials*. Brisbane, Australia.
- Kristombu Baduge, S., Mendis, P., & Ngo, T. (2013). Ductility design of high-strength reinforced concrete columns for super-tall buildings. In *Presented at the 4th international conference on structural engineering and construction management*. Kandy, Sri Lanka.
- Kristombu Baduge, S., Mendis, P., & Ngo, T. (2018b). Stress–strain relationship for very-high strength concrete (> 100 MPa) confined by lateral reinforcement. *Engineering Structures*, 177, 795–808. <https://doi.org/10.1016/j.engstruct.2018.08.008>.
- Kristombu Baduge, S., Mendis, P., Ngo, T., Fernando, W., & Waduge, B. (2015). Structural feasibility of very-high strength concrete (100–150 MPa) for tall buildings. In *Presented at the 6th international conference on structural engineering and construction management*, Sri Lanka.
- Kristombu Baduge, S., Mendis, P., Ngo, T., Portella, J., & Nguyen, K. (2018c). Understanding failure and stress–strain behavior of very-high strength concrete (> 100 MPa) confined by lateral reinforcement. *Construction and Building Materials*, 189, 62–77. <https://doi.org/10.1016/j.conbuildmat.2018.08.192>.
- Kwan, A. K. H., & Ho, J. C. M. (2010). Ductility design of high-strength concrete beams and columns. *Advances in Structural Engineering*, 13(4), 651–664.
- Lee, L., Vanissorn, V., Shanaka, K. B., Priyan, M., & Tuan, N. (2018). Properties of matrix, aggregate and interfacial transition zone in very high strength concrete (> 100 MPa) Using Nanoindentation Techniques. In *Presented at the international federation for structural concrete 5th international fib congress*.
- Légeron, F., & Paultre, P. (2000). Behavior of high-strength concrete columns under cyclic flexure and constant axial load. *ACI Structural Journal*, 97, 4.
- Légeron, F., & Paultre, P. (2003). Uniaxial confinement model for normal- and high-strength concrete columns. *Journal of Structural Engineering*, 129(2), 241.
- Li, B., Park, R., & Tanaka, H. (1991). Effect of confinement on the behaviour of high strength concrete columns under seismic loading. In *Proceedings, pacific conference on earthquake engineering, Auckland* (pp. 67–78).
- Mander, J. B., Priestley, M. J. N., & Park, R. (1984). *Seismic design of bridge piers*. New Zealand: University of Canterbury.
- Mander, J. B., Priestley, M. J. N., & Park, R. (1988). Theoretical stress–strain model for confined concrete. *Journal of Structural Engineering*, 114(8), 1804.
- MATLAB User's Guide. (1998). The mathworks. Inc., Natick, MA, 5, 333.
- Mau, S. T. (1990). Effect of tie spacing on inelastic buckling of reinforcing bars. *ACI Structural Journal*, 87, 6.
- Mau, S. T., & El-Mabsout, M. (1989). Inelastic buckling of reinforcing bars. *Journal of engineering mechanics*, 115(1), 1–17.
- Mendis, P. (2001a). *Design of high strength concrete members : state-of-the-art*. Engineers Australia.
- Mendis, P. (2001b). Plastic hinge lengths of normal and high-strength concrete in flexure. *Advances in Structural Engineering*, 4(4), 189–195.
- Mendis, P., & Kovacic, D. (1999). Spacing of stirrups for high-strength concrete columns in ordinary moment resisting frames. *Australian Journal of Structural Engineering*, 2(2/3), 95–104.
- Mendis, P., Kovacic, D. A., & Setunge, S. (2000a). Basis for the design of lateral reinforcement for high-strength concrete columns. *Structural Engineering and Mechanics*, 9(6), 589–600.
- Mendis, P., Pendyala, R., & Setunge, S. (2000b). Stress–strain model to predict the full-range moment curvature behaviour of high-strength concrete sections. *Magazine of Concrete Research*, 52(4), 227–234.
- Mitchell, D., & Paultre, P. (1994). Ductility and overstrength in seismic design of reinforced concrete structures. *Canadian Journal of Civil Engineering*, 21(6), 1049–1060.
- NZS 1170.5. (2004). *Structural design actions*. Wellington, N.Z.: Standards Association of New Zealand.
- NZS 3101.1. (2006). *Code of practice for the design of concrete structures NZ 3101*. Wellington: Standards Association of New Zealand.
- Papia, M., & Russo, G. (1989). Compressive concrete strain at buckling of longitudinal reinforcement. *Journal of Structural Engineering*, 115(2), 382–397.
- Park, R., & Paulay, T. (1975). *Reinforced concrete structures*. New York: Wiley.
- Park, R., Priestley, M. J., & Gill, W. D. (1982). Ductility of square-confined concrete columns. *Journal of the structural division*, 108(4), 929–950.
- Paultre, P., & Légeron, F. (2008). Confinement reinforcement design for reinforced concrete columns. *Journal of Structural Engineering*, 134(5), 738–749. [https://doi.org/10.1061/\(ASCE\)0733-9445\(2008\)134:5\(738\)](https://doi.org/10.1061/(ASCE)0733-9445(2008)134:5(738)).
- Paultre, P., Légeron, F., & Mongeau, D. (2001). Influence of concrete strength and transverse reinforcement yield strength on behavior of high-strength concrete columns. *ACI Structural Journal*, 98, 4.
- Razvi, S., & Saatcioglu, M. (1999). Confinement model for high-strength concrete. *Journal of Structural Engineering*, 125(3), 281.
- Saatcioglu, M., & Razvi, S. (1998). High-strength concrete columns with square sections under concentric compression. *Journal of Structural Engineering*, 124(12), 1438–1447. [https://doi.org/10.1061/\(ASCE\)0733-9445\(1998\)124:12\(1438\)](https://doi.org/10.1061/(ASCE)0733-9445(1998)124:12(1438)).
- Saatcioglu, M., & Razvi, S. R. (2002). Displacement-based design of reinforced concrete columns for confinement. *ACI Structural Journal*, 99(1). <http://www.concrete.org/Publications/InternationalConcreteAbstractsPortal.aspx?m=details&i=11030>. Accessed 25 May 2015.
- Samani, A. K., & Attard, M. M. (2012). A stress–strain model for uniaxial and confined concrete under compression. *Engineering Structures*, 41, 335–349. <https://doi.org/10.1016/j.engstruct.2012.03.027>.
- Samra, R. M. (1990). Ductility analysis of confined columns. *Journal of Structural Engineering*, 116(11), 3148–3161.
- Scribner, C. F. (1986). Reinforcement buckling in reinforced concrete flexural members. In *ACI journal proceedings* (Vol. 83). ACI.
- Sheikh, S. A., & Khoury, S. S. (1997). A performance-based approach for the design of confining steel in tied columns. *ACI Structural Journal*, 94, 4.
- Watson, S., Zahn, F., & Park, R. (1994). Confining reinforcement for concrete columns. *Journal of Structural Engineering*, 120(6), 1798–1824. [https://doi.org/10.1061/\(ASCE\)0733-9445\(1994\)120:6\(1798\)](https://doi.org/10.1061/(ASCE)0733-9445(1994)120:6(1798)).
- Wei, Y., & Wu, Y.-F. (2014). Compression behavior of concrete columns confined by high strength steel wire. *Construction and Building Materials*, 54, 443–453. <https://doi.org/10.1016/j.conbuildmat.2013.12.083>.

Publisher's Note

Springer Nature remains neutral with regard to jurisdictional claims in published maps and institutional affiliations.

Submit your manuscript to a SpringerOpen® journal and benefit from:

- Convenient online submission
- Rigorous peer review
- Open access: articles freely available online
- High visibility within the field
- Retaining the copyright to your article

Submit your next manuscript at ► springeropen.com